

# A Dirichlet-Multinomial-Poisson framework for the coherent analysis and forecast of cause-specific mortality

Andrea Nigri 

Department of Social Sciences  
University of Foggia

Han Lin Shang 

Department of Actuarial Studies and Business Analytics  
Macquarie University

Francesco Ungolo 

School of Risk and Actuarial Studies  
UNSW Sydney

## Abstract

Separate modelling of cause-specific mortality rates and their projections can yield inconsistent forecasts when the sum of deaths by cause does not match the total observed in a population. We develop a hierarchical probabilistic framework for cause-specific mortality counts in which both the total number of deaths and the occurrence of deaths across causes are treated as random. Conditional on the total number of deaths, cause-specific counts follow a multinomial distribution, whereas the total count is modelled using a Poisson distribution, and the vector of cause-of-death probabilities is assigned a Dirichlet distribution. The variation in cause-specific mortality rates by age and calendar year is captured in both the Poisson and Dirichlet models, allowing interpretable demographic patterns while preserving coherence by construction. This model construction naturally preserves the coherence between the sum of deaths by cause and the total mortality.

The method is exhibited through the analysis of cause-specific mortality rates in the United States and France, sourced from the Human Mortality Database from 1979 to 2023, separately by sex and across ages, with deaths grouped into major cause categories. The empirical analysis uses a rolling 15-year out-of-sample evaluation and compares the proposed model with the standard Lee–Carter model and its compositional extension. The results show that coherent projections can be obtained across countries and sexes, that competitive predictive accuracy is achieved, and that uncertainty is well-calibrated for both total and cause-specific mortality.

**Keywords:** Age-period model; Bayesian hierarchical modelling; Compositional count data; Dirichlet-Multinomial-Poisson model; Lee-Carter model

# 1 Introduction

Human life expectancy increased considerably in developed countries during the twentieth century due to improved living standards, medical advances, and advances in public health policies. For example, in the United States (U.S.), life expectancy at birth increased from 47.3 years in 1900 to 78.7 years in 2010 (Crimmins, 2015). This aspect poses profound epidemiological and social challenges. In addition to the ageing process, the impact of each cause of death changes over time. The proportion of deaths from some causes, such as infectious diseases, is declining dramatically due to medical advances, while others remain persistent or even increase. For public health decision makers, identifying the evolution of mortality by cause is highly relevant for guiding prevention strategies, allocating resources, and designing interventions targeting specific cohorts or generations (see, e.g., Preston et al., 2000; Booth and Tickle, 2008; Basellini et al., 2023).

Traditional approaches for extrapolating general mortality rates, such as the model of Lee and Carter (see Basellini et al., 2023, for a recent review), have proven very useful for capturing age-specific trends and projecting overall mortality rates. However, when used for separate analysis of mortality of subpopulations, or by cause of death, these models can produce forecasts that violate basic demographic constraints, such as the addition of cause-specific deaths to total mortality (see, e.g., Wilmoth, 1995; Hyndman et al., 2013). This incoherence yields implausible long-term projections and complicates their interpretation for policy purposes.

From a statistical perspective, modelling mortality by cause is far from trivial. Causes of death are, by definition, mutually exclusive and collectively exhaustive. Their compositional structure implies that independent modelling for each cause, as in the seminal work of Chiang (1991), may produce incoherent results, in which the sum of cause-specific forecasts exceeds or falls short of total mortality. This incoherence undermines both actuarial applications and the credibility of long-term public health scenarios, often producing more pessimistic forecasts (Wilmoth, 1995). A growing research strand has considered the compositional statistical analysis of the proportions of cause-of-death occurrences, embedding statistical frameworks that enforce coherence (see, e.g., Oeppen, 2008; Kjærsgaard et al., 2019; Cardillo et al., 2023, 2024, among others).

A promising development in this direction is the integration of a Dirichlet regression within age-specific mortality modelling. By assuming that the proportion of deaths by cause follows a Dirichlet

distribution, it is possible to directly account for the compositional nature of mortality without the need to resort to transformations, as in the work of [Zheng and Chen \(2017\)](#). Recent contributions show that this approach preserves interpretability while providing a coherent framework for capturing age and temporal variation across causes ([Graziani and Nigri, 2026](#)). Furthermore, the Dirichlet framework can be naturally combined with age–period (AP) and their age–period–cohort extensions.

The decomposition of age–period–cohort models unravels the biological effect of ageing, period shocks such as pandemics or medical innovations, and cohort effects reflecting the unique experiences of generations ([Renshaw and Haberman, 2006](#); [Hunt and Blake, 2014](#)). Extending this paradigm to causes of death enables researchers to uncover hidden regularities in mortality dynamics and improve overall forecasts.

Similar lines of research have focused on age–period models of mortality gaps, particularly when comparing major causes of death such as cancer and circulatory diseases. Using probabilistic models such as the Skellam distribution, these studies capture differences in mortality counts with a good degree of parsimony, highlighting the potential of age–period structures to analyse cause-specific disparities ([Li et al., 2019](#); [Lanfiuti Baldi et al., 2025](#)). Together, these works highlight a crucial methodological challenge: how to model both the level of total mortality and the composition of deaths by cause while retaining the flexibility to account for age- and period-specific dynamics.

This paper contributes to the literature by proposing a Dirichlet-Multinomial-Poisson (DMP) framework for analysing mortality rates by cause. This framework assumes that death counts by cause follow a multinomial distribution, where both the cause-specific probability of death and the total number of deaths are random and follow Dirichlet and Poisson distributions, respectively. This model induces a double source of dispersion, allowing for the capture of variation in the number of deaths and in the proportions of occurrences across causes. Both types of variation can be explained by covariates such as age and calendar year. The methodology is showcased in the analysis, and the forecast of the mortality rates by cause for the U.S. and France observed between 1979 and 2023. Such rates are analysed separately by sex, using a rolling holdout in which the rates over the last 15 years of the observation period are used to assess the predictive abilities of the two approaches. The results in the DMP framework of this paper are compared with the Lee–Carter

(LC) model applied to the analysis of mortality rates by each cause, and with the compositional data analysis (CoDa) method of [Kjærgaard et al. \(2019\)](#).

The model parameters under the DMP are estimated via a fully Bayesian analysis. This inferential strategy allows us to quantify the uncertainty of the projected rates. This aspect is relevant for policy and planning, as it allows one to assess the model's or parameter's uncertainty levels; compare the estimation or forecast accuracy of different methods more thoroughly; and explore different scenarios based on various assumptions ([Chatfield, 2000](#)).

The predictive uncertainty is obtained by construction from the joint generative model, and it naturally integrates (i) stochastic variability in future death counts and cause allocations and (ii) parameter uncertainty through the posterior distribution. This differs from classical approaches such as the LC model, fitted separately by cause, or CoDa methods applied to life-table quantities, where uncertainty bands are often introduced post-hoc, may not propagate all sources of uncertainty in a unified manner, and do not necessarily deliver coherent uncertainty statements simultaneously for totals and causes. By merging demographic reasoning with advanced statistical modelling, our approach simultaneously addresses the epidemiological need to monitor shifting cause-of-death patterns and the statistical demand for coherent and well-calibrated forecasts. This contribution is a step toward a general statistical framework that unifies mortality forecasting and cause-of-death analysis, with applications ranging from longevity risk management to health policy planning.

The remainder of the paper is structured as follows. Section 2 introduces the mortality modelling framework and the DMP framework and its application. Section 3 describes the Bayesian inferential framework. In Section 4, we present a forecasting framework using AP and LC models. Section 5 details the data used in the empirical analysis. Section 6 reports and discusses the results, and Section 7 concludes with final remarks and directions for future research.

## 2 Longevity Modelling

The statistical modelling of mortality rates captures the variation in three key dimensions: *age*, *period*, and *cause of death*. The age describes the biological and social processes that vary systematically throughout the life cycle; the period reflects contemporaneous shocks and innovations, such

as pandemics, wars, or medical advances, that affect all age groups simultaneously throughout a specific calendar year. Finally, the cause of death provides the epidemiological breakdown of mortality into mutually exclusive and collectively exhaustive categories.

To this end, let  $E_{a,t}$  denote the *exposure to risk* (person-years at risk), or age group  $a$  during period  $t$ , and let  $Y_{a,t}$  denote the random number of deaths among individuals aged  $a$  last birthday occurring during period  $t$  due to cause  $c$ . Therefore, the total number of deaths for the age group  $a$  and the period  $t$ ,  $Y_{a,t}$ , can be obtained as the sum of the number of deaths for each cause,  $Y_{a,t} = \sum_c Y_{a,t,c}$ .

For each age  $a$ , year  $t$ , and cause of death  $c$ , the researcher observes the following:

- $E_{at}$ : the population *exposure to risk*, often approximated by the average between the population aged  $a$  at the start of the period  $t$  and the population aged  $a$  at the end of the same period;
- $Y_{atc}$ : the number of *deaths* observed at age  $a$ , year  $t$ , due to cause  $c$ .

The corresponding *central death rate* is defined as

$$m_{a,t,c} = \frac{Y_{a,t,c}}{E_{a,t}}, \quad (1)$$

which represents the cause  $c$  average mortality intensity at age  $a$  in year  $t$ . In demographic and actuarial analyses, this quantity is used as an unbiased estimator of the *force of mortality*  $\mu(a, t, c)$ , namely the instantaneous risk of death at exact age  $a$  and calendar time  $t$  by cause  $c$  (Preston et al., 2000):

$$m_{a,t,c} \approx \mu(x, t, c), \quad x \in [a, a + 1). \quad (2)$$

For this reason, following the early literature (see, e.g., Brouhns et al., 2002), it is assumed that the random number of deaths  $Y_{a,t,c}$  follows a Poisson distribution with mean and variance depending on the central death rate as follows:

$$Y_{a,t,c} \sim \text{Poisson}(E_{a,t} m_{a,t,c}).$$

This formulation ensures that cause-specific deaths aggregate coherently with the total number

of deaths. By the reproducibility property of the Poisson distribution, the sum of the cause-specific death counts is also Poisson-distributed:

$$\sum_c Y_{a,t,c} = Y_{a,t} \sim \text{Poisson}(E_{a,t} m_{a,t}), \quad (3)$$

where  $m_{a,t} = \sum_c m_{a,t,c}$ .

The proposed DMP framework consists of a hierarchical model, where: i) the total number of deaths  $Y_{a,t}$  follows a Poisson distribution, and ii) the vector of the number of deaths by each cause  $\bar{Y}_{a,t} = (Y_{a,t,1}, \dots, Y_{a,t,C})$  follows a Dirichlet-Multinomial (DM) distribution (Mosimann, 1962). The causes of death are listed for ease of exposition in Table 2. The DM distribution is indexed by two parameters, namely the total number of deaths  $Y_{a,t}$  and a vector  $\bar{\alpha}_{a,t} = \phi \bar{\gamma}_{a,t}$ , where  $\bar{\gamma}_{a,t} = (\gamma_{a,t,1}, \dots, \gamma_{a,t,C})$ , such that  $\sum_c \gamma_{a,t,c} = 1$ , and  $\phi$  controls the overdispersion of  $\bar{\gamma}_{a,t}$ . Thus,  $\bar{Y}_{a,t} \sim \text{DM}(\bar{\alpha}_{a,t}, Y_{a,t})$ , with probability mass function

$$p(\bar{y}_{a,t} | \bar{\alpha}_{a,t}, y_{a,t}) = \frac{\Gamma(\phi) \Gamma(y_{a,t} + 1)}{\Gamma(y_{a,t} + \phi)} \prod_{c=1}^C \frac{\Gamma(y_{a,t,c} + \phi \gamma_{a,t,c})}{\Gamma(\phi \gamma_{a,t,c}) \Gamma(y_{a,t,c} + 1)},$$

where  $\Gamma(\cdot)$  denotes the Gamma function.

This construction ensures that the cause-specific mortality hazard decomposes as  $m_{a,t,c} = m_{a,t} \gamma_{a,t,c}$ , which aligns the mean structure of the Dirichlet-Multinomial model with the overall mortality hazard  $m_{a,t}$  and the compositional proportions  $\gamma_{a,t}$ . Each probability  $\gamma_{a,t,c}$  is modelled in terms of a softmax function as follows:

$$\gamma_{a,t,c} = \frac{\exp(\eta_{a,t,c})}{\sum_c \exp(\eta_{a,t,c})}. \quad (4)$$

Where  $\eta_{a,t,c}$  is a latent linear predictor for cause  $c$  at age  $a$  and year  $t$ .

The DM model combines the Multinomial distribution with Dirichlet-distributed probabilities. In this way, it is possible to account for overdispersion in the vector of cause-specific death counts and to account for the evolution of this composition over the years due to medical and societal advancements. In addition, since the Dirichlet distribution is supported on the simplex, the resulting model ensures compositional coherence and offers a flexible tool for probabilistic

modelling and forecasting.

For the data described in Section 5, two models are considered for the rate of the Poisson distribution  $m_{a,t}$ , and for the argument of the softmax function  $\eta_{atc}$  to derive the underlying probability of the DM model, namely the AP model in Section 2.1 and the LC model in Section 2.2.

## 2.1 Age-Period model

This model assumes that age and period are two factors that proportionally affect the rate of the Poisson distribution:

$$\log m_{a,t} = \nu_0 + \delta_a + \pi_t, \quad (5)$$

where  $\nu_0$  is the baseline log-mortality rate, and  $\delta_a$  is the factor deviation corresponding to the effect associated with age  $a$ , and  $\pi_t$  is the proportional effect due to calendar year  $t$ . Similarly, age and period have an additive effect on the parameter  $\eta_{a,t,c}$  through the parameters  $\zeta_{a,c}$  and  $\lambda_{t,c}$ , respectively, for cause  $c$  as deviation from the baseline parameter  $\varphi_{0,c}$ :

$$\eta_{a,t,c} = \varphi_{0,c} + \zeta_{a,c} + \lambda_{t,c}. \quad (6)$$

Mortality rates typically evolve smoothly across ages and over calendar years, and the same pattern is observed in the cause-specific probabilities of death. To reflect this empirical regularity and to avoid overfitting, a smoothing effect is imposed on the parameters  $\delta_a$ ,  $\pi_t$ ,  $\eta_{a,c}^c$ , and  $\eta_t^c$  ( $c = 1, \dots, C$ ). This strategy improves the stability of estimates in sparsely populated cells and captures the gradual demographic and epidemiological transitions commonly seen in mortality data. To this end, each effect is modelled as a second-order Gaussian random walk (RW2, [Bryant and Zhang \(2018\)](#)):

$$\Delta^2 \delta_a \equiv \delta_a - 2\delta_{a-1} + \delta_{a-2} \stackrel{\text{iid}}{\sim} \mathcal{N}(0, \sigma_\delta^2), \quad a \geq 3 \quad (7)$$

$$\Delta^2 \pi_t \equiv \pi_t - 2\pi_{t-1} + \pi_{t-2} \stackrel{\text{iid}}{\sim} \mathcal{N}(0, \sigma_\pi^2), \quad t \geq 3$$

$$\Delta^2 \zeta_{a,c} \equiv \zeta_{a,c} - 2\zeta_{a-1,c} + \zeta_{a-2,c} \stackrel{\text{iid}}{\sim} \mathcal{N}(0, \sigma_\zeta^2), \quad a \geq 3 \quad (8)$$

$$\Delta^2 \lambda_{t,c} \equiv \lambda_{t,c} - 2\lambda_{t-1,c} + \lambda_{t-2,c} \stackrel{\text{iid}}{\sim} \mathcal{N}(0, \sigma_\lambda^2), \quad t \geq 3.$$

For  $a = 1, 2$  and  $t = 1, 2$ , age- and period-specific parameters are free parameters to be inferred through the Bayesian inferential procedure outlined in Section 3.

## 2.2 Lee-Carter model

This model assumes that the log-rate of the Poisson distribution is given by the sum of a baseline mortality level  $\nu_0$ , an age-specific factor  $\delta_a$ , and an age-period interaction effect<sup>1</sup>:

$$\log m_{a,t} = \nu_0 + \delta_a + \beta_a \kappa_t. \quad (9)$$

To ensure the identifiability of the model parameters, the classical LC constraints are imposed (Hunt and Blake, 2014):

$$\sum_{t=1}^T \kappa_t = 0, \quad \sum_{a=1}^A \beta_a = 1.$$

The age effect  $\delta_a$  is smoothed by assuming a RW2 process as in equation (7), while for the LC model,  $\kappa_t$  is assumed to follow a first-order random walk (RW1):

$$(\kappa_t \mid \kappa_{t-1}) \sim \mathcal{N}(\kappa_{t-1}, \sigma_\kappa^2), \quad t \geq 2.$$

The parameter  $\eta_{a,t,c}$  is modelled as an additive function of the age and of a cause-period interaction term. More precisely, such an interaction component uses the same calendar year effect  $\kappa_t$  as used in the log-rate of the Poisson model.

This approach allows for the capture of systematic reallocations of the total number of deaths across causes:

$$\eta_{a,t,c} = \varphi_{0,c} + \zeta_{a,c} + \vartheta_c \kappa_t,$$

where  $\zeta_{a,c}$  is an age-by-cause smooth deviation and  $\vartheta_c$  is a cause-specific loading to measure the interaction between cause of death probability and period.

The cause-period interaction uses the same calendar-year effect  $\kappa_t$  as in the Poisson log-rate. In

---

<sup>1</sup>This parameterisation is algebraically equivalent to the classical LC model ( $a_a = \nu_0 + \delta_a$ ,  $b_a = \beta_a$ ). In our approach, this reparameterisation is useful because it separates the global mortality level ( $\nu_0$ ) from the age profile ( $\delta_a$ ), facilitates centred and smoothed priors on age effects, and improves MCMC stability while preserving the same mean structure. Identification is enforced by  $\sum_a \delta_a = 0$ ,  $\sum_t \kappa_t = 0$ , and  $\sum_a \beta_a = 1$ .

the LC–DM model, Poisson and Dirichlet–Multinomial parameters are estimated *jointly* in a single Bayesian hierarchy (i.e., no two-stage plug-in for  $\kappa_t$ ), as made explicit by the joint likelihood in Section 3.

The age cause-specific effect  $\zeta_{a,c}$  is also smoothed through an RW2 process as in (8).

### 3 Inference

#### 3.1 Prior distribution

The statistical analysis of the cause-specific mortality rates in Section 5 is conducted under non-informative prior assumptions. All parameters are assumed to be pairwise independent *a priori*, so that prior information does not impose artificial dependencies across the components of the model.

Hence, diffuse priors are assigned to the intercepts and level parameters governing total mortality and the cause-specific compositions. The prior distribution for each model parameter under the AP and LC specifications is summarised in Table 1.

Table 1: Prior specifications and identifiability constraints for the AP–DM and LC–DM models.

| Model block  | Parameter(s)               | Prior / Constraint        |
|--|----------------------------|---------------------------|
| <b>AP–DM: total mortality (Poisson)</b>  |                            |                           |
|  | $\nu_0$                    | $\mathcal{N}(0, 5^2)$     |
|  | $\delta_1, \delta_2$       | $\mathcal{N}(0, 5^2)$     |
|  | $\pi_1, \pi_2$             | $\mathcal{N}(0, 1)$       |
|  | $\sigma_\delta$            | $\mathcal{N}^+(0, 1^2)$   |
|  | $\sigma_\pi$               | $\mathcal{N}^+(0, 0.3^2)$ |
| <b>AP–DM: composition (Dirichlet–Multinomial), for each cause <math>c = 1, \dots, C</math></b> |                            |                           |
|  | $\varphi_{0,c}$            | $\mathcal{N}(0, 5^2)$     |
|  | $\zeta_{1,c}, \zeta_{2,c}$ | $\mathcal{N}(0, 5^2)$     |

Continued on next page

| Model block  | Parameter(s)                   | Prior / Constraint  |
|--|--------------------------------|---|
|  | $\lambda_{1,c}, \lambda_{2,c}$ | $\mathcal{N}(0, 1)$   |
|  | $\sigma_\zeta$                 | $\mathcal{N}^+(0, 1^2)$   |
|  | $\sigma_\lambda$               | $\mathcal{N}^+(0, 0.3^2)$   |
| <b>AP-DM: overdispersion</b>   |                                |   |
|  | $\phi$                         | $\log \mathcal{N}(\phi_\mu, \phi_\sigma)$   |
| <b>AP-DM: identifiability constraints</b>  |                                |   |
|  |                                | $\sum_{a=1}^A \delta_a = 0, \sum_{t=1}^T \pi_t = 0, \sum_{c=1}^C \varphi_{0,c} = 0,$<br>$\sum_{a=1}^A \zeta_{a,c} = 0, \sum_{t=1}^T \lambda_{t,c} = 0 \ (\forall c).$ |
| <b>LC-DM: total mortality (LC + Poisson)</b>   |                                |   |
|  | $\nu_0$                        | $\mathcal{N}(0, 10^2)$  |
|  | $\delta_1, \delta_2$           | $\mathcal{N}(0, 5^2)$   |
|  | $\beta_a$                      | $\mathcal{N}^+(0, 1^2)$   |
|  | $\kappa_1$                     | $\mathcal{N}(0, 1^2)$   |
|  | $\sigma_\delta$                | $\mathcal{N}^+(0, 0.5^2)$   |
|  | $\sigma_\kappa$                | $\mathcal{N}^+(0, 0.5^2)$   |
| <b>LC-DM: composition (Dirichlet-Multinomial), for each cause <math>c = 1, \dots, C</math></b> |                                |   |
|  | $\varphi_{0,c}$                | $\mathcal{N}(0, 1^2)$   |
|  | $\zeta_{1,c}, \zeta_{2,c}$     | $\mathcal{N}(0, 1^2)$   |
|  | $\vartheta_c$                  | $\mathcal{N}(0, 0.5^2)$   |
|  | $\sigma_\zeta$                 | $\mathcal{N}^+(0, 0.4^2)$   |
| <b>LC-DM: overdispersion</b>   |                                |   |
|  | $\phi$                         | $\log \mathcal{N}(\phi_\mu, \phi_\sigma)$   |
| <b>LC-DM: identifiability constraints</b>  |                                |   |
|  |                                | $\sum_{t=1}^T \kappa_t = 0, \sum_{a=1}^A \beta_a = 1, \sum_{a=1}^A \delta_a = 0,$<br>$\sum_{c=1}^C \varphi_{0,c} = 0, \sum_{a=1}^A \zeta_{a,c} = 0 \ (\forall c).$    |

The model includes a small set of parameters (e.g., intercepts, dispersion, and cause-specific loadings), while the remaining parameters are indexed by age and period (e.g.,  $\delta_a, \beta_a, \kappa_t, \zeta_{a,c}$ ). Therefore, the total dimension depends on the data and increases with the number of ages ( $A$ ) and periods ( $T$ ) considered.

These choices aim to minimise the influence of prior specification on posterior inference, allowing the data to fully determine the posterior distribution of the parameters.

### 3.2 Likelihood

Let  $\theta$  denote the full vector of model parameters indexing the DMP under the assumptions of the AP or LC model. For each age group  $a$  and calendar year  $t$ , the observed death counts are conditionally independent given the corresponding parameters.

The likelihood function for  $\theta$ , conditional on exposures  $E_{a,t}$  and observed death counts by cause  $\mathbf{Y}$ , factorises into a Poisson component for total deaths and a DM component for the cause composition:

$$\mathcal{L}(\theta; \mathbf{Y}, \mathbf{E}) = \prod_{a=1}^A \prod_{t=1}^T \underbrace{p(\mathbf{y}_{a,t} | E_{a,t} \mathbf{m}_{a,t})}_{\text{Poisson}(E_{a,t} \mathbf{m}_{a,t})} \times \underbrace{p(\bar{\mathbf{y}}_{a,t} | \phi \bar{\mathbf{y}}_{a,t}, \mathbf{y}_{a,t})}_{\text{DM}(\phi \bar{\mathbf{y}}_{a,t}, \mathbf{y}_{a,t})}, \quad (10)$$

where  $\bar{\mathbf{y}}_{a,t} = (y_{a,t,1}, \dots, y_{a,t,C})$ ,  $\mathbf{y}_{a,t} = \sum_{c=1}^C y_{a,t,c}$ , and  $\theta$  can be  $\theta_{\text{AP}} = \{\nu_0, \delta, \pi, \phi, \zeta, \lambda, \sigma_\delta, \sigma_\pi, \sigma_\zeta, \sigma_\lambda\}$ ,  $\theta_{\text{LC}} = \{\nu_0, \delta, \beta, \kappa, \phi, \zeta, \vartheta, \sigma_\delta, \sigma_\kappa, \sigma_\zeta\}$ .

The Poisson component governs the uncertainty around the total number of deaths, while the Dirichlet–Multinomial component captures the allocation of these deaths across causes and accommodates overdispersion and compositional structure.

### 3.3 Posterior inference

Posterior inference follows from the product of the likelihood in Section 3.2 and the prior specification densities, as outlined in Section 3.1. The resulting posterior distribution does not admit a closed-form expression.

The posterior distribution of the parameters is estimated using the Hamiltonian Monte Carlo (HMC) algorithm, a class of Metropolis-Hastings samplers that enables faster, more effective

exploration of the parameter space. This is implemented in Stan (Stan Development Team, 2025) through the  interface using the  package `rstan`. The sampler is automatically tuned through the “no U-turns sampler” of Hoffman and Gelman (2014). The key feature of the HMC sampler is the ability to generate proposals that follow informed trajectories through the parameter space, taking advantage of the geometry of the target density. This results in more efficient exploration, particularly in high-dimensional parameter spaces with highly correlated parameters, thereby reducing autocorrelation and accelerating convergence.

## 4 Projection

Let  $H$  denote the forecast horizon and  $\mathcal{T}^+ = \{T+1, \dots, T+H\}$  the set of future periods. The primary goal is to obtain coherent projections of age-specific mortality rates by cause such that the sum of cause-specific rates equals the corresponding total rate at each age and period. This ensures epidemiological interpretability and avoids incoherence between aggregate and disaggregate forecasts.

If official population projections are available, exposures  $E_{a,t}$  for  $t \in \mathcal{T}^+$  can be incorporated to produce forecasts of future death counts. However, the fundamental outputs of our model are forecasts on the *rate scale*: the total death rate  $m_{a,t}$  and the vector of cause-specific shares  $\gamma_{a,t,c}$ . This strategy guarantees that the forecasts remain internally consistent across causes, even when exposures are unknown or uncertain.

**Forecasting under AP-DM.** Future-period effects can be obtained by leveraging their assumed RW2 dynamics beyond  $T$ . For each posterior draw and  $t \in \mathcal{T}^+$ ,

$$\begin{aligned}\pi_t &= 2\pi_{t-1} - \pi_{t-2} + \varepsilon_t^{(\pi)}, & \varepsilon_t^{(\pi)} &\sim \mathcal{N}(0, \sigma_\pi^2), \\ \lambda_{t,c} &= 2\lambda_{t-1,c} - \lambda_{t-2,c} + \varepsilon_{t,c}^{(\lambda)}, & \varepsilon_{t,c}^{(\lambda)} &\sim \mathcal{N}(0, \sigma_\lambda^2), \quad c = 1, \dots, C.\end{aligned}$$

The age effects  $\delta_a$  and  $\zeta_{a,c}$  remain fixed, with centring constraints applied for numerical stability.

Therefore, the projected total rate  $m_{a,t}$  and the corresponding cause shares  $\gamma_{a,t,c}$  are computed

as follows:

$$m_{a,t} = \exp\{\nu_0 + \delta_a + \pi_t\}, \quad \gamma_{a,t,c} = \frac{\exp\{\varphi_{0,c} + \zeta_{a,c} + \lambda_{t,c}\}}{\sum_{c'} \exp\{\varphi_{0,c'} + \zeta_{a,c'} + \lambda_{t,c'}\}}, \quad \sum_c \gamma_{a,t,c} = 1.$$

**Forecasting under LC–DM.** For LC–DM we simulate the future  $\kappa_t$  by extending the RW1 dynamics:

$$\kappa_t = \kappa_{t-1} + \varepsilon_t^{(\kappa)}, \quad \varepsilon_t^{(\kappa)} \sim \mathcal{N}(0, \sigma_\kappa^2), \quad t \in \mathcal{T}^+.$$

The age effects  $\delta_a$  and  $\zeta_{ac}$  remain fixed (with centering constraints), while  $\beta_a$  and  $\vartheta_c$  are time-invariant loadings.

For LC–DM, the corresponding projected quantities are

$$m_{at} = \exp\{\nu_0 + \delta_a + \beta_a \kappa_t\}, \quad \gamma_{atc} = \frac{\exp\{\varphi_{0,c} + \zeta_{a,c} + \vartheta_c \kappa_t\}}{\sum_{c'} \exp\{\varphi_{0,c'} + \zeta_{a,c'} + \vartheta_{c'} \kappa_t\}}, \quad \sum_c \gamma_{atc} = 1.$$

For both AP and LC models, the combination of these projected quantities directly yields cause-specific mortality rates  $m_{a,t,c} = m_{a,t} \gamma_{a,t,c}$ , which are coherent by construction, since  $\sum_c m_{atc} = m_{at}$  for all  $(a, t)$ . Thus, forecasts naturally provide both the aggregate dynamics and their decomposition across causes <sup>2</sup>.

## 5 Data

The models outlined in Section 2 are showcased through an analysis of mortality rates, as available in [Human Mortality Database \(2026\)](#). These are extracted from the period life tables by sex and 5-year age group (0–100+) of the HMD from 1979 to 2023. Death counts by cause and exposure are sourced from [Human Cause-of-death Data series \(2026\)](#) (HCD) for both gender in the U.S. and France, and the proportions of deaths by cause, age, and calendar year are computed. The HCD Database provides high-quality cause-specific mortality data in five-year age groups. The taxonomy of the causes of death is given by the International Classification of Diseases (ICD) of

<sup>2</sup>If exposures  $E_{a,t}$  are available, predictive counts can be simulated via

$$Y_{a,t} \sim \text{Poisson}(E_{a,t} m_{a,t}), \quad \bar{Y}_{a,t} \sim \text{DM}(\phi \bar{Y}_{a,t}),$$

with  $\sum_c Y_{a,t,c} = Y_{a,t}$  by design.

the World Health Organisation and consists of three aggregation levels: full list, intermediate list, and short list. Each classification has been developed using the same criteria across all countries, ensuring its homogeneity and comparability. Using these data, one can develop a universal and standardised methodology to redistribute deaths across 104 disease categories within five-year age groups, avoiding issues due to ICD revisions and ensuring cross-country comparability despite differing coding practices. Starting with the HCD classification, the main causes of death are grouped by age up to 100+.

To understand the conditions that may have affected the life expectancy of the U.S. population, six major causes have been considered: Infectious, neoplasms, cardiovascular diseases (CVDs), respiratory diseases, external diseases, and ‘other’, which includes all remaining causes. Table 2 summarises the information on cause-groups by the ICD10 classification system.

Table 2: ICD codes and classification into six broad categories.

| Title   | ICD 10              | Cause       |
|---|---------------------|-------------|
| Infectious  | A00–B99             | Infectious  |
| Neoplasms   | C00–D48             | Neoplasms   |
| Heart diseases  | I00–I52             | CVD         |
| Cerebrovascular diseases                                  | G45, I60–I69        | CVD         |
| Other and unspecified disorders of the circulatory system | I70–I99             | CVD         |
| Acute respiratory diseases                                | J00–J22, U04        | Respiratory |
| Other respiratory diseases                                | J30–J98             | Respiratory |
| External causes   | V01–Y98             | External    |
| All other causes  | Remaining ICD codes | Other       |

Data from 1989–2008 (1989–2007 for France) are used to estimate the posterior distribution of the model parameters, while the remaining data (2009–2023 for the U.S. and 2008–2022 for France) are used as held-out set to assess the predictive performance of the proposed approach, using a 15-year window for both countries. In a second modelling exercise, whose results are reported in Appendix A, the data from 1979 until 1988 are also used to fit the model, and the predictive performance is again assessed over the period 2009–2023 for the U.S. and 2008–2022 for France.

The HMC sampler described in Section 3.3 was run three times in parallel, yielding three chains each with 3,000 samples, where the first 1,500 draws were used as a warm-up. The convergence of the posterior distribution of the parameters was assessed through the  $\hat{R}$  diagnostic in Tables 15 and 16, (see, e.g., Gelman and Rubin, 1992; Stan Development Team, 2025).

## 6 Results

First of all, for most parameters the  $\widehat{R}$  is below the suggested 1.05 threshold, indicating that the three chains converged towards a stationary posterior distribution.

Posterior summaries for the scalar parameter of the Bayesian AP and LC models, by sex and in-sample year in both countries under analysis, are presented in Appendix C.

Let  $\log \widehat{m}_{a,t,c}$  denote the predicted value of  $\log m_{a,t,c}$ , namely the death rate in log scale for age  $a$ , year  $t$ , cause  $c$  under the model considered. The accuracy over the evaluation set  $\mathcal{J}$  (all  $(a, t, c)$  in the out-of-sample years) is assessed by calculating the mean absolute error (MAE) and the root mean squared error (RMSE):

$$\begin{aligned} \text{MAE} &= \frac{1}{|\mathcal{J}|} \sum_{(a,t,c) \in \mathcal{J}} |\log m_{a,t,c} - \log \widehat{m}_{a,t,c}|, \\ \text{RMSE} &= \left[ \frac{1}{|\mathcal{J}|} \sum_{(a,t,c) \in \mathcal{J}} (\log m_{a,t,c} - \log \widehat{m}_{a,t,c})^2 \right]^{1/2}. \end{aligned}$$

Both measures are calculated also separately by cause, together with their correspondent in-sample summaries, and then compared with those obtainable under the LC model fitted by each cause singly, and with the CoDA approach. The key features of these two competing approaches are summarised in Appendix B.

### 6.1 United States (U.S.)

The DMP-AP, DMP-LC, CoDa, and LC are compared under a rolling 15-year out-of-sample evaluation. Table 3 shows the in-sample (Train) and the out-of-sample (OOS) MAE and RMSE by sex for the total number of deaths.

**Total mortality** Table 3 shows a clear advantage for the DMP-LC specification on the total mortality surface. For both females and males, DMP-LC achieves the lowest in-sample and out-of-sample errors. This is consistent with the role of the latent period index in capturing the dominant secular trend while borrowing strength across ages through the smooth age structure. DMP-AP typically ranks next among the coherent Bayesian specifications, indicating that an additive age–

period structure remains competitive. The LC factorisation yields a sharper representation of the time trend in this application.

Table 3: U.S. – Total mortality performance (Train vs OOS) by sex. Lower is better. Best in **bold**, second best underlined (within each sex).

| Sex     | Model  | Train RMSE    | Train MAE     | OOS RMSE      | OOS MAE       |
|---------|--------|---------------|---------------|---------------|---------------|
| Females | DMP-AP | <u>0.0084</u> | <u>0.0027</u> | 0.0208        | 0.0072        |
|         | DMP-LC | <b>0.0047</b> | <b>0.0015</b> | <b>0.0090</b> | <b>0.0039</b> |
|         | CoDa   | 0.1475        | 0.0833        | 0.1464        | 0.0808        |
|         | LC     | 0.0101        | 0.0034        | <u>0.0134</u> | <u>0.0047</u> |
| Males   | DMP-AP | 0.0174        | 0.0058        | 0.0199        | 0.0074        |
|         | DMP-LC | <b>0.0038</b> | <b>0.0015</b> | <b>0.0110</b> | <b>0.0051</b> |
|         | CoDa   | 0.1690        | 0.1011        | 0.1663        | 0.0944        |
|         | LC     | <u>0.0158</u> | <u>0.0055</u> | <u>0.0179</u> | <u>0.0070</u> |

By contrast, the LC benchmark (fitted independently in each series in our implementation) is consistently less accurate than DMP-LC on totals, despite being the second-best method overall on aggregate metrics in several cells. This suggests that the Bayesian formulation, with explicit smoothing priors and joint inference, offers a real gain over the classical LC baseline. The CoDa approach exhibits substantially larger errors in total mortality under this evaluation, which is unsurprising given that CoDa methods are designed to model death distributions in a life-table (simplex) geometry rather than directly modelling death rates.

**Mortality by cause** Table 4 shows the out-of sample RMSE and MAE by sex and cause. The results are heterogeneous across causes, but two empirical patterns are notable. The DMP-AP and DMP-LC models are systematically among the top performers (best or second-best) for several major causes, and they do so while preserving internal coherence between totals and causes. In particular, DMP-LC is competitive for neoplasms (NEOP) in both sexes and performs strongly for cardiovascular diseases (CVD) in males on RMSE. At the same time, DMP-AP remains competitive for CVD, looking at the MAE and for external causes (EXT) in females. These findings are consistent with the intention of the modelling. Indeed, DMP-LC uses a single latent time factor to drive both the overall mortality level and systematic reallocations across causes. In contrast, DMP-AP allows for a more flexible (additive) period component in both the total and the composition.

In addition, the cause-specific LC and the CoDa can perform better when analysing specific

causes, yet these gains do not translate uniformly across the full system. This is an important distinction: specifically, when the LC is fitted independently by cause (a common practice), it does not guarantee coherence between the sum of cause-specific forecasts and the forecast of total mortality, potentially producing internally inconsistent projections. [Kjærgaard et al. \(2019\)](#) discuss this general limitation of independently forecasting cause-specific rates and motivate coherent alternatives that respect the competing-risk structure. In a similar manner, CoDa methods enforce coherence in the compositional (life-table deaths) space by construction, but they operate on transformed life-table quantities (e.g., centred log-ratio (CLR)-transformed life-table deaths) and require an additional layer of analysis; these features can make performance sensitive to the particular evaluation target (rates vs. life-table deaths) and to data idiosyncrasies, especially for smaller causes.

Table 4: U.S. – Out-of-sample performance by cause and model, with sex shown as column groups. Lower is better for RMSE/MAE. Best in **bold**, second best underlined (within each cause × sex, separately for RMSE and MAE).

| Cause | Model  | Females       |               | Males         |               |
|-------|--------|---------------|---------------|---------------|---------------|
|       |        | RMSE          | MAE           | RMSE          | MAE           |
| CVD   | DMP-AP | <b>0.0060</b> | <u>0.0024</u> | 0.0132        | <b>0.0042</b> |
|       | DMP-LC | 0.0134        | 0.0056        | <b>0.0112</b> | 0.0052        |
|       | CoDa   | <u>0.0066</u> | <b>0.0020</b> | 0.0146        | <u>0.0050</u> |
|       | LC     | 0.0158        | 0.0068        | <u>0.0124</u> | 0.0061        |
| EXT   | DMP-AP | <b>0.0004</b> | <b>0.0002</b> | 0.0008        | 0.0004        |
|       | DMP-LC | <u>0.0004</u> | <u>0.0002</u> | <b>0.0004</b> | <u>0.0003</u> |
|       | CoDa   | 0.0004        | 0.0002        | 0.0007        | 0.0004        |
|       | LC     | 0.0017        | 0.0007        | <u>0.0005</u> | <b>0.0003</b> |
| INF   | DMP-AP | 0.0006        | 0.0002        | 0.0012        | 0.0006        |
|       | DMP-LC | 0.0005        | 0.0002        | <u>0.0008</u> | <u>0.0004</u> |
|       | CoDa   | <b>0.0002</b> | <b>0.0001</b> | 0.0012        | 0.0005        |
|       | LC     | <u>0.0004</u> | <u>0.0002</u> | <b>0.0004</b> | <b>0.0002</b> |
| NEOP  | DMP-AP | 0.0024        | 0.0011        | 0.0030        | 0.0013        |
|       | DMP-LC | <b>0.0007</b> | <b>0.0004</b> | <u>0.0023</u> | <u>0.0013</u> |
|       | CoDa   | 0.0011        | <u>0.0005</u> | <b>0.0017</b> | <b>0.0007</b> |

continued on next page

| Cause | Model  | Females       |               | Males         |               |
|-------|--------|---------------|---------------|---------------|---------------|
|       |        | RMSE          | MAE           | RMSE          | MAE           |
| OTHER | LC     | <u>0.0008</u> | 0.0005        | 0.0023        | 0.0014        |
|       | DMP-AP | <u>0.0081</u> | <u>0.0032</u> | <u>0.0080</u> | <b>0.0029</b> |
|       | DMP-LC | 0.0100        | 0.0035        | <b>0.0076</b> | <u>0.0030</u> |
|       | CoDa   | <b>0.0069</b> | <b>0.0023</b> | 0.0095        | 0.0036        |
| RESP  | LC     | 0.0279        | 0.0105        | 0.0310        | 0.0127        |
|       | DMP-AP | 0.0080        | 0.0026        | 0.0058        | 0.0021        |
|       | DMP-LC | 0.0044        | 0.0016        | 0.0056        | 0.0022        |
|       | CoDa   | <u>0.0035</u> | <b>0.0010</b> | <b>0.0044</b> | <b>0.0017</b> |
|       | LC     | <b>0.0033</b> | <u>0.0012</u> | <u>0.0046</u> | <u>0.0019</u> |

Table 5 summarises arithmetic averages of RMSE and MAE by causes. For males, the RMSE is lowest for the DMP-LC model, while the MAE is lowest for the DMP-AP model. These results indicate that the coherent Bayesian approaches offer the best overall trade-off when aggregating the two measures of predictive performance across the causes. For females, the CoDa model yields the lowest mean errors across causes. However, this result should be treated with caution. In the overall analysis, the same method performs poorly for all-cause mortality under the current rate-based metric. This suggests that the compositional life-table model is optimising something different from what is being evaluated here.

Table 5: U.S. – OOS mean performance across causes by sex. Lower is better. Best in **bold**, second best underlined (within each sex).

| Sex    | Model  | RMSE mean     | MAE mean      |
|--------|--------|---------------|---------------|
| Female | DMP-AP | <u>0.0042</u> | <u>0.0016</u> |
|        | DMP-LC | 0.0049        | 0.0019        |
|        | CoDa   | <b>0.0031</b> | <b>0.0010</b> |
|        | LC     | 0.0083        | 0.0033        |
| Male   | DMP-AP | <u>0.0053</u> | <b>0.0019</b> |
|        | DMP-LC | <b>0.0047</b> | 0.0021        |
|        | CoDa   | 0.0054        | <u>0.0020</u> |
|        | LC     | 0.0085        | 0.0038        |

In contrast, DMP-LC produces the most accurate total mortality forecasts while remaining

competitive across multiple causes, which is precisely the objective of coherent forecasting in applications where both the level and the decomposition of mortality rates are of relevance.

These results support two conclusions. 1) The Bayesian LC–DM formulation provides the most accurate forecasts for total mortality in both sexes over the forecast horizon, while maintaining coherence between total and cause-specific rates by construction. 2) Although some benchmarks can outperform our models for specific causes, they do not deliver the same combination of (i) accurate totals, (ii) coherent decomposition, and (iii) a single joint probabilistic model that yields predictive uncertainty for both the level and the composition. This joint/coherent perspective is essential for public-health planning, because internally inconsistent cause forecasts can lead to implausible decompositions even when individual cause trajectories appear reasonable (Kjærgaard et al., 2019).

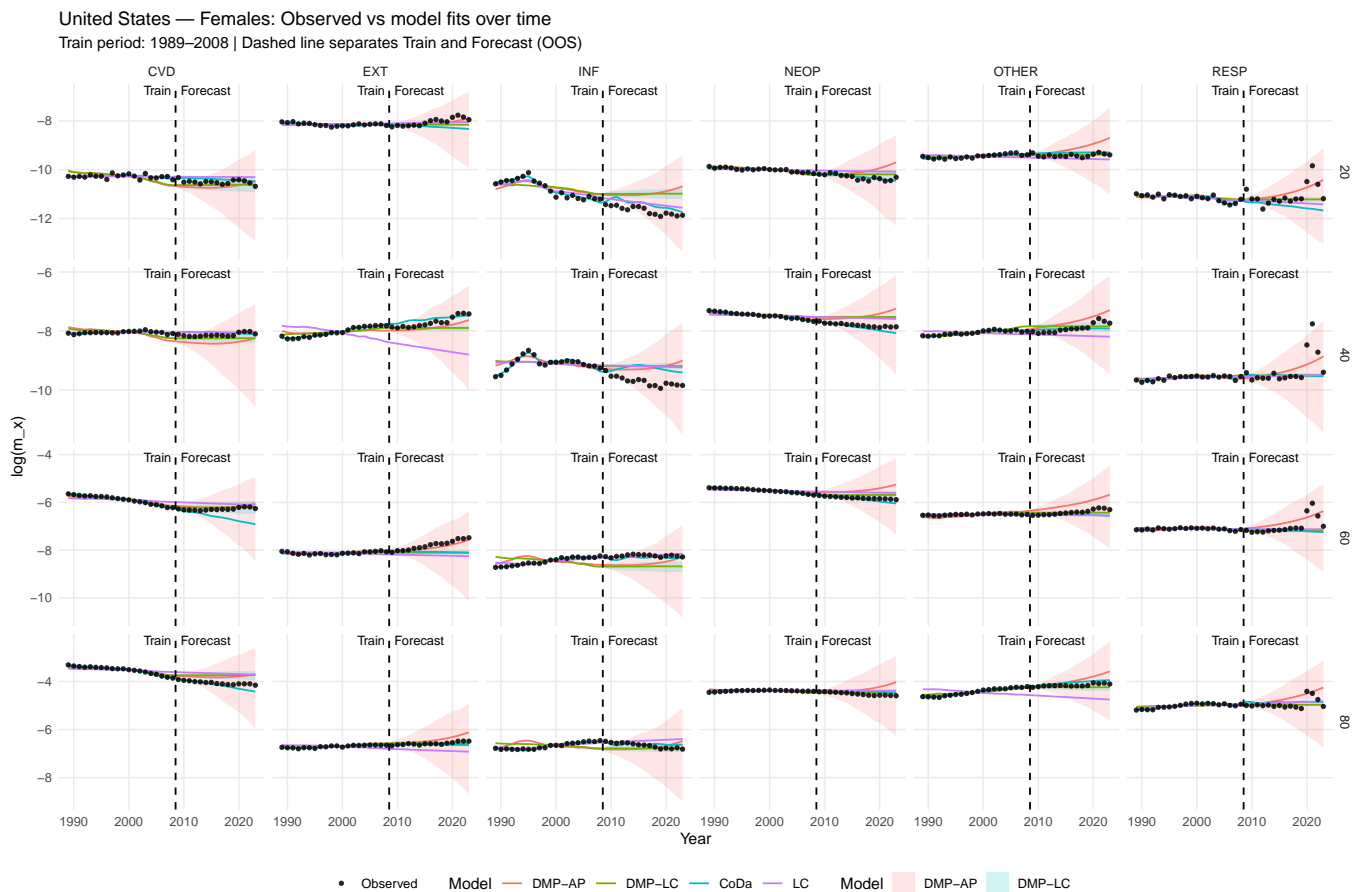


Figure 1: U.S. Female: Observed (black points) and fitted/forecast log mortality rates by cause for selected ages (20, 40, 60, 80). The vertical dashed line marks the end of the in-sample period (1989–2008) and the start of the out-of-sample forecasts.

Figures 1 and 2 display the observed log-mortality rates by cause over time for selected ages (20,

40, 60, 80), with the vertical dashed line marking the transition from the in-sample window (1989–2008) to the forecasting window. The observed rates (black dots) are generally fitted well by the two coherent DMP specifications (DMP-AP and DMP-LC). Their predictive intervals widen after 2008, reflecting the increasing uncertainty over the forecast horizon. This behaviour is particularly evident in causes with higher variability and/or weaker signals at young ages, where credible intervals expand substantially in OOS.

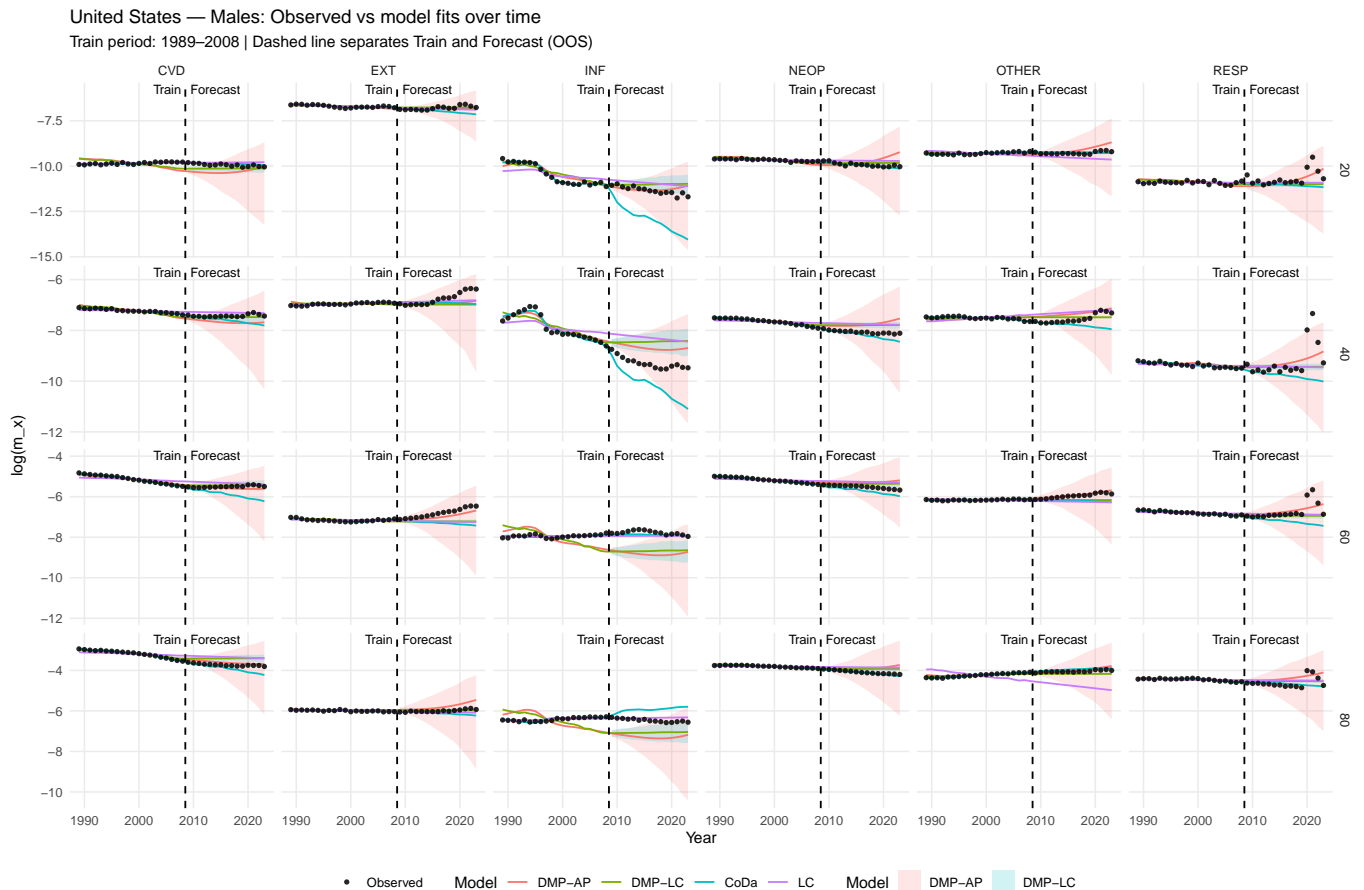


Figure 2: U.S. Male: Observed (black points) and fitted/forecast log mortality rates by cause for selected ages (20, 40, 60, 80). The vertical dashed line marks the end of the in-sample period (1989–2008) and the start of the out-of-sample forecasts.

Across both sexes, DMP-LC tends to provide the most stable extrapolations in panels dominated by smooth trends (e.g., CVD and NEOP at older ages), while DMP-AP remains competitive when the post-2008 dynamics resemble a continuation of the pre-2008 additive period pattern. In contrast, the non-coherent benchmarks can display more pronounced panel-specific departures in OOS. The single-cause LC fits sometimes show systematic drift relative to the observed points in certain age–cause combinations, and CoDa exhibits occasional strong deviations in some infectious/respiratory panels (notably at younger ages), consistent with sensitivity to the life-table/compositional

representation when evaluated on rate trajectories.

Overall, the plots support the previous findings: coherent Bayesian models provide excellent in-sample calibration, plausible and more competitive out-of-sample trajectories, and uncertainty bands that expand appropriately beyond the in-sample boundary, while maintaining internally consistent cause decompositions at each age and period.

## 6.2 France

We report results for France using the same evaluation design as for the U.S.: the last 15 calendar years are held out as out-of-sample, and the preceding years form the in-sample set. Performance is evaluated on (i) the total mortality surface and (ii) cause-specific mortality, using RMSE and MAE (lower is better), reported separately by sex in Tables 6–8.

Table 6 shows that the DMP-LC specification dominates total mortality forecasting for both sexes in France when in-sample starts in 1989. For females, DMP-LC achieves the lowest in-sample and out-of-sample errors, with a substantial gap over the alternatives. A striking feature is the very large OOS error in DMP-AP for females on totals, indicating an unstable extrapolation of the level component over the forecast horizon. For males, DMP-LC is again the most accurate method regarding totals, followed by the classical LC benchmark, while CoDa remains clearly less competitive on the rate scale in this aggregate evaluation.

Table 6: France – Total mortality performance (Train vs OOS) by sex, train from 1989. Lower is better. Best in **bold**, second best underlined (within each sex, separately for each metric).

| Sex     | Model  | Train RMSE    | Train MAE     | OOS RMSE      | OOS MAE       |
|---------|--------|---------------|---------------|---------------|---------------|
| Females | DMP-AP | 0.0092        | 0.0027        | 0.2826        | 0.0647        |
|         | DMP-LC | <b>0.0036</b> | <b>0.0010</b> | <b>0.0074</b> | <b>0.0028</b> |
|         | CoDa   | 0.1527        | 0.0838        | 0.1413        | 0.0738        |
|         | LC     | <u>0.0057</u> | <u>0.0022</u> | <u>0.0094</u> | <u>0.0046</u> |
| Males   | DMP-AP | 0.0160        | 0.0047        | 0.0324        | 0.0121        |
|         | DMP-LC | <b>0.0078</b> | <b>0.0022</b> | <b>0.0100</b> | <b>0.0045</b> |
|         | CoDa   | 0.1784        | 0.1048        | 0.1624        | 0.0910        |
|         | LC     | <u>0.0087</u> | <u>0.0034</u> | <u>0.0129</u> | <u>0.0069</u> |

Table 7 details the performance of OOS by cause. The picture is heterogeneous, but two patterns emerge. First, DMP-LC is consistently among the top performers in most causes for both sexes,

while preserving the coherence between the total and cause decomposition by construction. In particular, DMP-LC is best for males in cardiovascular diseases (CVD), external causes (EXT), and residual category (OTHER) for RMSE and MAE, and it remains highly competitive for neoplasms (NEOP). For females, DMP-LC is best for EXT and OTHER, and near-best for CVD and infectious diseases (INF), confirming that a single latent time index can capture both the dominant trend and systematic reallocations across causes.

Table 7: France – Out-of-sample performance by cause and model, train from 1989, with sex shown as column groups. Lower is better for RMSE/MAE. Best in **bold**, second best underlined (within each cause × sex, separately for RMSE and MAE).

| Cause | Model  | Females       |               | Males         |               |
|-------|--------|---------------|---------------|---------------|---------------|
|       |        | RMSE          | MAE           | RMSE          | MAE           |
| CVD   | DMP-AP | 0.0752        | 0.0178        | 0.0117        | 0.0046        |
|       | DMP-LC | <u>0.0055</u> | <u>0.0023</u> | <b>0.0064</b> | <b>0.0029</b> |
|       | CoDa   | <b>0.0038</b> | <b>0.0010</b> | 0.0129        | <u>0.0039</u> |
|       | LC     | 0.0094        | 0.0042        | <u>0.0092</u> | 0.0045        |
| EXT   | DMP-AP | 0.0217        | 0.0047        | 0.0046        | 0.0015        |
|       | DMP-LC | <b>0.0008</b> | <b>0.0003</b> | <b>0.0013</b> | <b>0.0004</b> |
|       | CoDa   | 0.0017        | 0.0005        | 0.0016        | <u>0.0005</u> |
|       | LC     | <u>0.0011</u> | <u>0.0005</u> | <u>0.0013</u> | 0.0005        |
| INF   | DMP-AP | 0.0052        | 0.0012        | 0.0016        | 0.0006        |
|       | DMP-LC | <b>0.0004</b> | <u>0.0002</u> | <u>0.0013</u> | 0.0005        |
|       | CoDa   | 0.0007        | 0.0002        | 0.0017        | <u>0.0005</u> |
|       | LC     | <u>0.0005</u> | <b>0.0002</b> | <b>0.0005</b> | <b>0.0002</b> |
| NEOP  | DMP-AP | 0.0462        | 0.0123        | 0.0085        | 0.0029        |
|       | DMP-LC | <u>0.0008</u> | <u>0.0003</u> | <b>0.0020</b> | <u>0.0011</u> |
|       | CoDa   | 0.0015        | 0.0007        | 0.0028        | <b>0.0010</b> |
|       | LC     | <b>0.0007</b> | <b>0.0003</b> | <u>0.0024</u> | 0.0015        |
| OTHER | DMP-AP | 0.0932        | 0.0210        | 0.0086        | 0.0029        |
|       | DMP-LC | <b>0.0033</b> | <b>0.0009</b> | <b>0.0022</b> | <b>0.0008</b> |
|       | CoDa   | <u>0.0038</u> | <u>0.0012</u> | 0.0053        | 0.0016        |
|       | LC     | 0.0047        | 0.0014        | <u>0.0031</u> | <u>0.0011</u> |

continued on next page

| Cause | Model  | Females       |               | Males         |               |
|-------|--------|---------------|---------------|---------------|---------------|
|       |        | RMSE          | MAE           | RMSE          | MAE           |
| RESP  | DMP-AP | 0.0443        | 0.0080        | <b>0.0046</b> | <b>0.0014</b> |
|       | DMP-LC | <b>0.0043</b> | <b>0.0011</b> | 0.0071        | <u>0.0019</u> |
|       | CoDa   | 0.0058        | 0.0015        | 0.0120        | 0.0033        |
|       | LC     | <u>0.0043</u> | <u>0.0012</u> | <u>0.0069</u> | 0.0021        |

Second, the benchmark methods can be strong for specific causes but do not dominate uniformly. For example, CoDa is best for females in CVD (both RMSE and MAE) and performs competitively in several other female causes, while the classical LC benchmark is best for females in NEOP and for INF (notably on MAE), and it is also competitive for males in INF. As in the analysis of the U.S. data, such cause-by-cause gains should be interpreted alongside system-level coherence: independently fitted LC models (one per cause) do not guarantee that cause-specific forecasts sum to the forecast of total mortality, whereas both Bayesian specifications enforce coherence at each age and period.

The averages over causes in Table 8 reinforce these conclusions. For males, DMP-LC attains the lowest mean RMSE and mean MAE across causes. For females, DMP-LC has the lowest mean RMSE, and CoDa attains the lowest mean MAE, while DMP-AP is an outlier due to very large errors in multiple causes and, especially, regarding the total.

Table 8: France – OOS mean performance across causes, train from 1989, by sex. Lower is better. Best in **bold**, second best underlined (within each sex, separately for RMSE mean and MAE mean).

| Sex    | Model  | RMSE mean     | MAE mean      |
|--------|--------|---------------|---------------|
| Female | DMP-AP | 0.0476        | 0.0108        |
|        | DMP-LC | <b>0.0025</b> | <u>0.0009</u> |
|        | CoDa   | <u>0.0029</u> | <b>0.0008</b> |
|        | LC     | 0.0034        | 0.0013        |
| Male   | DMP-AP | 0.0066        | 0.0023        |
|        | DMP-LC | <b>0.0034</b> | <b>0.0013</b> |
|        | CoDa   | 0.0061        | 0.0018        |
|        | LC     | <u>0.0039</u> | <u>0.0016</u> |

Figures 3 and 4 provide a visual check of these results by showing observed log-mortality rates, fitted trajectories, and forecast behaviour for selected ages (20, 40, 60, 80), with the dashed

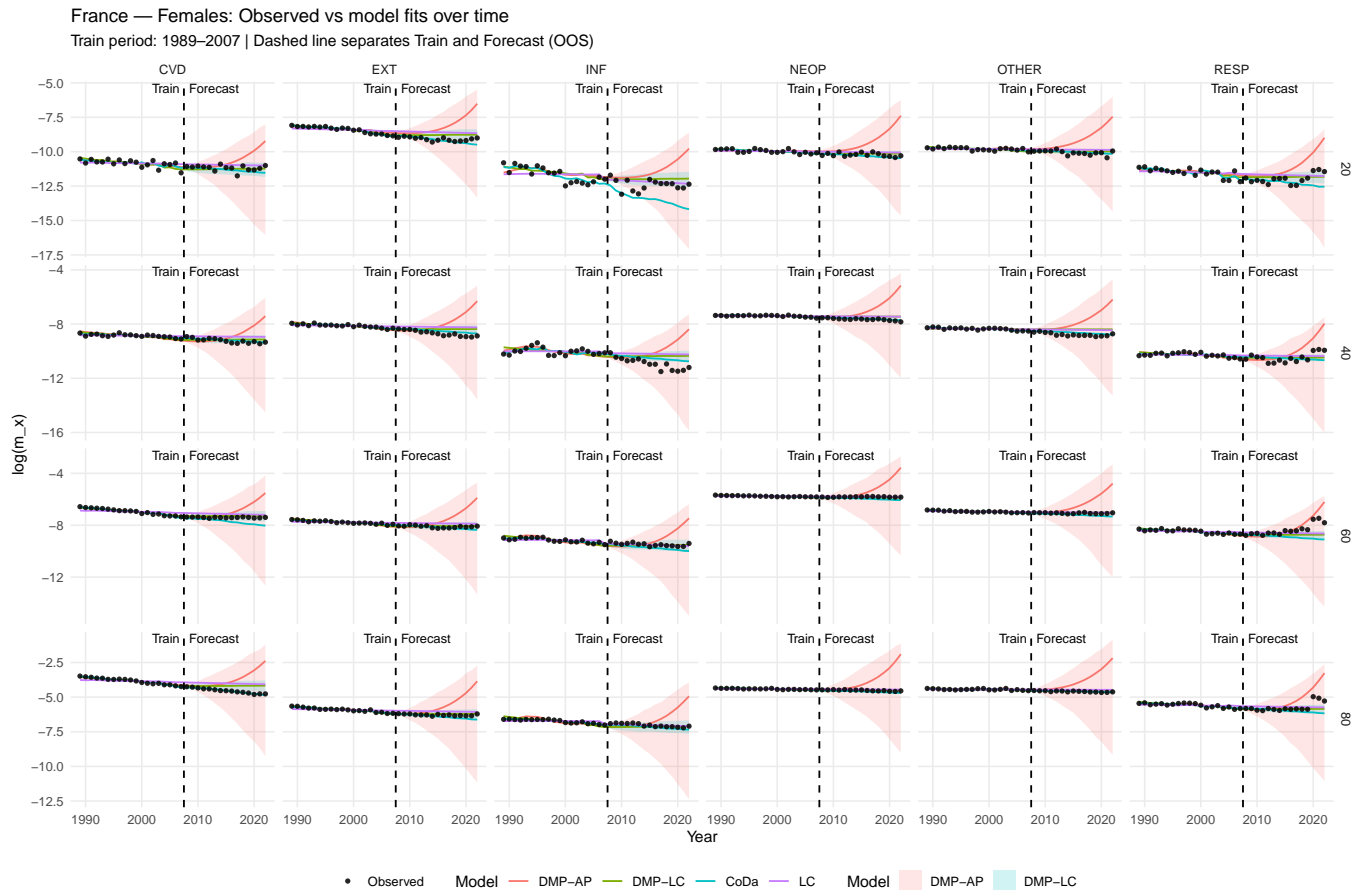


Figure 3: France Female: Observed (black points) and fitted/forecast log mortality rates by cause for selected ages (20, 40, 60, 80). The vertical dashed line marks the end of the in-sample period (1989–2007) and the start of the out-of-sample forecasts.

line marking the transition from in-sample (1989–2007) to OOS forecasting (2008 onwards). The plots show that DMP-LC closely tracks the pre-2008 trends and produces stable extrapolations after 2007, with uncertainty bands that widen gradually with the forecast horizon. In contrast, DMP-AP displays very wide predictive intervals and noticeable drift in several panels (particularly for females), consistent with poor OOS performance on totals and across multiple causes. This behaviour is in line with a highly flexible period component whose second-order random-walk extrapolation can generate rapidly increasing uncertainty and curvature over longer horizons. CoDa and LC remain competitive in selected cause–age panels (notably INF and NEOP), but their strengths are not uniform across the full cause partition, and they do not provide the same combination of accurate totals, coherent decomposition, and joint probabilistic uncertainty for both level and composition delivered by the coherent Bayesian formulations.

In the Appendix A, Tables 9–14 show the evaluation using a longer in-sample window starting

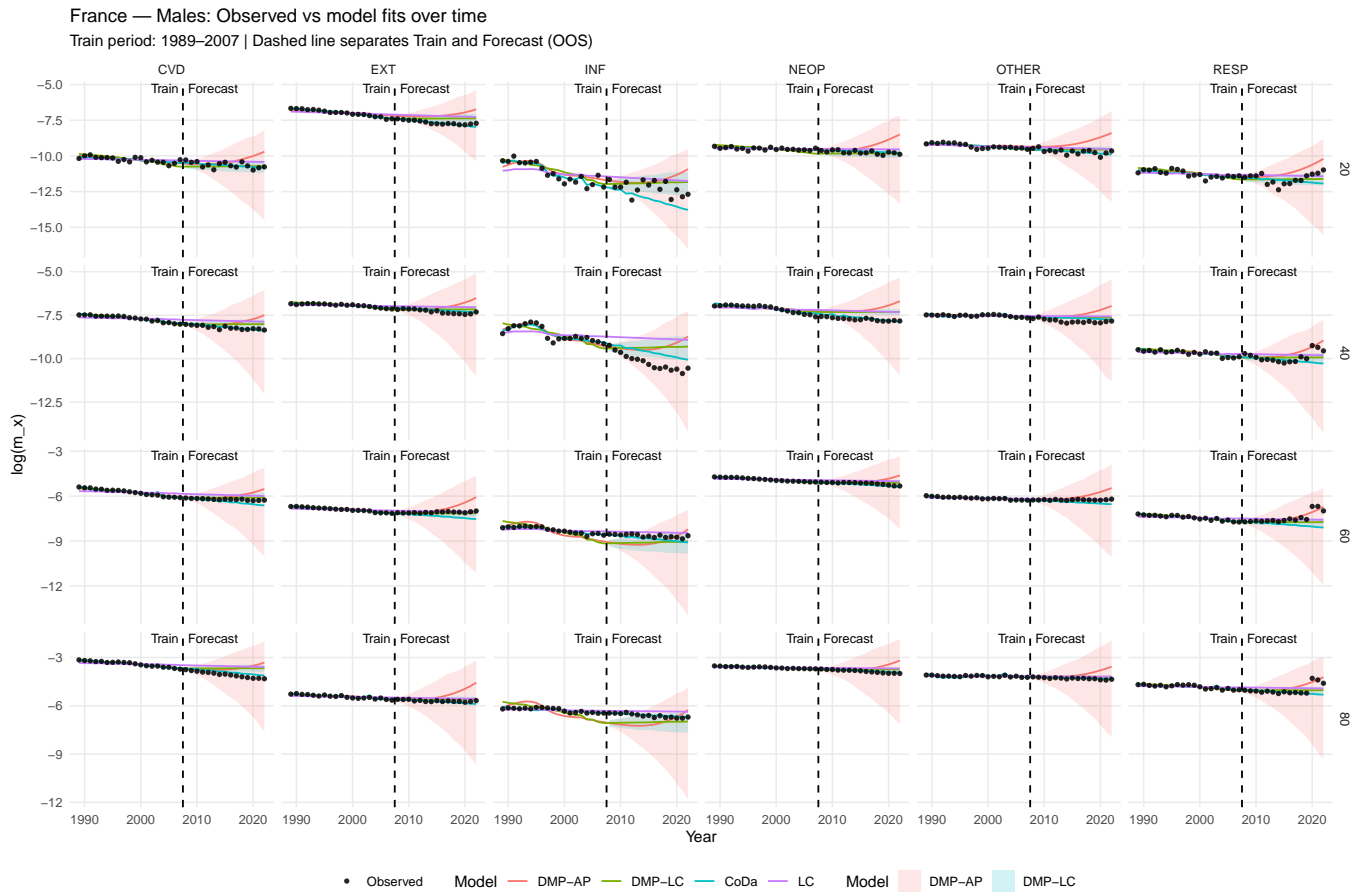


Figure 4: France Male: Observed (black points) and fitted/forecast log mortality rates by cause for selected ages (20, 40, 60, 80). The vertical dashed line marks the end of the in-sample period (1989–2007) and the start of the out-of-sample forecasts.

in 1979. For both countries, DMP-LC still provides the best performance on total mortality in both sexes, confirming the robustness of the LC-based coherent Bayesian specification when the estimation sample is expanded. In contrast, CoDa remains clearly less competitive overall in this rate-based evaluation, despite occasionally strong performance on specific causes.

For cause-specific performance, the longer in-sample window amplifies the heterogeneity already observed in the main text. In the U.S. data, CoDa often achieves the lowest averaged errors over causes (Table 13), while DMP-AP/DMP-LC remain consistently competitive and typically dominate for totals. In France, the same pattern appears. Indeed, CoDa yields the lowest average errors across causes for females, whereas DMP-LC is the best overall for males and remains among the top performers by cause (Table 14). Overall, the appendix results reinforce the main conclusion: coherent Bayesian models, especially DMP-LC, offer the most reliable accuracy for total mortality while maintaining a coherent composition structure, whereas benchmark methods may excel for

selected causes but do not match this system-level performance uniformly.

Overall, the estimation starting from 1979 confirms two robust findings: 1) DMP-LC provides the most stable and accurate total mortality forecasts across countries and sexes, and its advantage persists when the estimation window is substantially extended. 2) Cause-performance remains heterogeneous and depends on the evaluation target. Specifically, CoDa can excel for several individual causes and can even minimise errors across causes in some contexts, such as the female population; nevertheless, it performs poorly on totals. This reinforces the proposed methodological approaches, emphasising that the coherent Bayesian joint models (DMP-AP and especially DMP-LC) deliver a stronger forecast—accurate totals, coherent decomposition, and a single probabilistic description of uncertainty. In contrast, benchmark approaches may provide cause-specific gains that do not generalise to the full competing-risks/compositional system.

## 7 Conclusion

This paper introduces a Dirichlet–Multinomial–Poisson modelling framework for the analysis and forecasting of mortality by cause of death. The proposed hierarchical specification provides a modular structure in which the variation in total mortality by age and calendar year is modelled jointly with the allocation of deaths by causes. Randomness in both the total number of deaths and the cause-specific probabilities allows the model to capture age- and time-dependent dynamics in overall mortality and in the relative importance of different causes.

By modelling these components simultaneously, the framework delivers coherent forecasts of cause-specific mortality rates that are fully consistent with projections of all-cause mortality. Importantly, coherence is preserved not only at the level of point forecasts but also in the associated uncertainty, as dependence across causes is explicitly represented. The resulting approach offers a tractable and interpretable alternative to independent cause-specific models, while retaining analytical transparency and compatibility with Bayesian inference.

These benefits come at a cost. Full Bayesian estimation across the dimensions of age, period and cause can be computationally demanding and requires careful prior specification and diagnostic assessment, moreover, long-horizon projections may be sensitive to the assumed time structure. Empirically, the backtesting analysis for the United States and France highlights the importance of

coherent joint modelling. The LC-based coherent Bayesian specification (DMP-LC) achieves the lowest or near-lowest out-of-sample error on the aggregate mortality surface across countries and sexes, while remaining stable over longer horizons. In particular, for France, the latent period index plays a pivotal role in capturing the dominant secular trend and borrowing strength across ages within a coherent multi-cause system. At the cause-specific level, DMP-LC attains low RMSE across most causes and populations, avoids systematic bias, and preserves the aggregation constraint linking causes to totals. Competing approaches may outperform in isolated cases, but they do not simultaneously guarantee coherence between aggregate and disaggregate forecasts, nor provide joint predictive distributions for totals and causes. When internal consistency and interpretable predictive uncertainty are central, the coherent Bayesian framework offers a favourable trade-off between accuracy, coherence, and uncertainty quantification.

Several extensions merit further investigation. First, the Dirichlet concentration parameter could be allowed to vary across age or period, enabling greater flexibility in the dispersion of the compositional component. Second, additional over-dispersion or cohort structure could be introduced to assess whether such features provide incremental predictive value beyond period dynamics. While both extensions are feasible, their adoption should be guided by a careful cost-benefit assessment: additional computational and modelling complexity should be justified by tangible improvements in calibration, coherence, or forecast accuracy in the intended applications.

## **Acknowledgment**

Andrea Nigri thanks the insightful comments and suggestions from seminar participants at the School of Demography, Australian National University, and at the Department of Actuarial Studies and Business Analytics, Macquarie University.

## References

- U. Basellini, C. G. Camarda, and H. Booth. Thirty years on: A review of the Lee–Carter method for forecasting mortality. *International Journal of Forecasting*, 39(3):1033–1049, 2023.
- H. Booth and L. Tickle. Mortality modelling and forecasting: A review of methods. *Annals of Actuarial Science*, 3(1-2):3–43, 2008.
- N. Brouhns, M. Denuit, and J. K. Vermunt. A Poisson log-bilinear regression approach to the construction of projected lifetables. *Insurance: Mathematics and Economics*, 31(3):373–393, 2002.
- J. Bryant and J. L. Zhang. *Bayesian Demographic Estimation and Forecasting*. Chapman & Hall/CRC Press, Boca Raton, FL, 2018.
- G. Cardillo, P. Giordani, S. Levantesi, A. Nigri, and A. Spelta. Mortality forecasting using the four-way CANDECOMP/PARAFAC decomposition. *Scandinavian Actuarial Journal*, 2023(9): 916–932, 2023.
- G. Cardillo, P. Giordani, S. Levantesi, and A. Nigri. A tensor-based approach to cause-of-death mortality modeling. *Annals of Operations Research*, 342(3):2075–2094, 2024.
- C. Chatfield. *Time-Series Forecasting*. Chapman & Hall, Boca Raton, 2000.
- C. L. Chiang. Competing risks in mortality analysis. *Annual Review of Public Health*, 12(1):281–307, 1991.
- E. M. Crimmins. Lifespan and healthspan: Past, present, and promise. *The Gerontologist*, 55(6): 901–911, 2015.
- A. Gelman and D. B. Rubin. Inference from iterative simulation using multiple sequences. *Statistical Science*, 7(4):457–472, 1992.
- R. Graziani and A. Nigri. An age–period–cohort model in a Dirichlet framework: A coherent causes of death estimation. *Insurance: Mathematics and Economics*, 126:103194, 2026.
- M. D. Hoffman and A. Gelman. The no-u-turn sampler: Adaptively setting path lengths in hamiltonian monte carlo. *Journal of Machine Learning Research*, 15(1):1593–1623, 2014.

- Human Cause-of-death Data series. *Human Mortality Database*. Max Planck Institute for Demographic Research (Germany), University of California, Berkeley (USA), and French Institute for Demographic Studies (France), 2026. Available at [www.mortality.org](http://www.mortality.org) (data downloaded on 26-June-2024).
- Human Mortality Database. *University of California, Berkeley, USA; Max Planck Institute for Demographic Research, Germany*, 2026. Available online at the address <http://www.mortality.org> [accessed 26-June-2024].
- A. Hunt and D. Blake. A general procedure for constructing mortality models. *North American Actuarial Journal*, 18(1):116–138, 2014.
- R. J. Hyndman, H. Booth, and F. Yasmeeen. Coherent mortality forecasting: the product-ratio method with functional time series models. *Demography*, 50:261–283, 2013.
- S. Kjærgaard, Y. E. Ergemen, M. Kallestrup-Lamb, J. Oeppen, and R. Lindahl-Jacobsen. Forecasting causes of death by using compositional data analysis: the case of cancer deaths. *Journal of the Royal Statistical Society Series C: Applied Statistics*, 68(5):1351–1370, 2019.
- G. Lanfiuti Baldi, A. Nigri, and H. L. Shang. Age–period modeling of mortality gaps: The cases of cancer and circulatory diseases. *Journal of Official Statistics*, 41(4):1154–1180, 2025.
- R. D. Lee and L. R. Carter. Modeling and forecasting U.S. mortality. *Journal of the American Statistical Association: Applications & Case Studies*, 87(419):659–671, 1992.
- H. Li, H. Li, Y. Lu, and A. Panagiotelis. A forecast reconciliation approach to cause-of-death mortality modeling. *Insurance: Mathematics and Economics*, 86:122–133, 2019.
- J. E. Mosimann. On the compound multinomial distribution, the multivariate  $\beta$ -distribution, and correlations among proportions. *Biometrika*, 49(1 and 2):65–82, 1962.
- J. Oeppen. Coherent forecasting of multiple-decrement life tables: A test using Japanese cause of death data. In *European Association for Population Studies*, 2008. URL: <https://epc2008.eaps.nl/papers/80611>.
- S. Preston, P. Heuveline, and M. Guillot. *Demography: Measuring and Modeling Population Processes*. Blackwell Publishers, Malden, MA, 2000.

- A. E. Renshaw and S. Haberman. A cohort-based extension to the Lee–Carter model for mortality reduction factors. *Insurance: Mathematics and economics*, 38(3):556–570, 2006.
- Stan Development Team. Stan modeling language users guide and reference manual. <https://mc-stan.org/docs/stan-users-guide/index.html>, 2025. Version 2.38.
- J. R. Wilmoth. Are mortality projections always more pessimistic when disaggregated by cause of death? *Mathematical Population Studies*, 5(4):293–319, 1995.
- T. Zheng and R. Chen. Dirichlet ARMA models for compositional time series. *Journal of Multivariate Analysis*, 158:31–46, 2017.

## A U.S. and France, 1979

Tables 9–13 and 10–14 report a robustness check in which the in-sample window is extended back to 1979 (keeping the same 15-year OOS horizon). This experiment is informative because the longer estimation sample spans additional epidemiological phases and structural shifts, thereby stress-testing the extrapolation behaviour of the competing models.

Table 9: U.S. – Total mortality performance (Train vs OOS) by sex, train from 1979. Lower is better. Best in **bold**, second best underlined (within each sex, separately for each metric).

| Sex     | Model  | Train         |               | OOS           |               |
|---------|--------|---------------|---------------|---------------|---------------|
|         |        | RMSE          | MAE           | RMSE          | MAE           |
| Females | DMP-AP | 0.0132        | 0.0039        | <u>0.0184</u> | <u>0.0069</u> |
|         | DMP-LC | <b>0.0044</b> | <b>0.0014</b> | <b>0.0101</b> | <b>0.0042</b> |
|         | CoDa   | 0.1446        | 0.0831        | 0.1458        | 0.0804        |
|         | LC     | <u>0.0070</u> | <u>0.0030</u> | 0.0406        | 0.0178        |
| Males   | DMP-AP | <u>0.0254</u> | <u>0.0084</u> | <u>0.0290</u> | <u>0.0102</u> |
|         | DMP-LC | <b>0.0046</b> | <b>0.0017</b> | <b>0.0127</b> | <b>0.0058</b> |
|         | CoDa   | 0.1657        | 0.1016        | 0.1668        | 0.0951        |
|         | LC     | 0.1177        | 0.0257        | 0.0565        | 0.0219        |

Table 10: France – Total mortality performance (Train vs OOS) by sex, train from 1979. Lower is better. Best in **bold**, second best underlined (within each sex, separately for each metric).

| Sex     | Model  | Train         |               | OOS           |               |
|---------|--------|---------------|---------------|---------------|---------------|
|         |        | RMSE          | MAE           | RMSE          | MAE           |
| Females | DMP-AP | 0.0175        | 0.0048        | 0.1376        | 0.0354        |
|         | DMP-LC | <b>0.0040</b> | <b>0.0012</b> | <b>0.0074</b> | <b>0.0028</b> |
|         | CoDa   | 0.1594        | 0.0894        | 0.1403        | 0.0730        |
|         | LC     | <u>0.0127</u> | <u>0.0056</u> | <u>0.1011</u> | <u>0.0259</u> |
| Males   | DMP-AP | 0.0215        | 0.0068        | 0.0247        | 0.0100        |
|         | DMP-LC | <b>0.0082</b> | <b>0.0023</b> | <b>0.0108</b> | <b>0.0047</b> |
|         | CoDa   | 0.1869        | 0.1114        | 0.1603        | 0.0889        |
|         | LC     | <u>0.0161</u> | <u>0.0072</u> | <u>0.0270</u> | <u>0.0157</u> |

Across both countries and sexes, the rankings by total are remarkably stable. Indeed, DMP-LC remains overall the best-performing method in-sample and out-of-sample. For the U.S. (Table 9), DMP-LC attains the lowest OOS errors for both females and males, with DMP-AP generally second-best and the benchmarks (LC and especially CoDa) substantially less competitive on total

rates. France shows the same ordering for males (Table 10). For French females, DMP-LC again dominates, while DMP-AP and LC exhibit much larger OOS errors, indicating that the additive AP specification can remain sensitive in this setting even when trained on a longer historical window. Overall, extending the in-sample period strengthens the interpretation that the LC-based coherent Bayesian specification provides the most reliable system-level forecasts, in the sense of simultaneously modelling the level and maintaining a coherent decomposition.

At the cause level, the longer in-sample window accentuates the heterogeneity already visible in the main text. In the U.S. (Table 11), CoDa and LC can be best for specific causes (e.g., INF often favours CoDa/LC; EXT can favour LC for females), while DMP-LC is frequently competitive and often best for key male causes such as CVD. DMP-AP remains close to the best methods in several cells (especially for CVD females), suggesting that an additive age–period structure can still capture important movements in the composition, but its system-level advantage is not as robust as DMP-LC when the target is accurate totals plus coherence.

Table 11: U.S. – Out-of-sample performance by cause and model, train from 1979, with sex shown as column groups. Lower is better for RMSE/MAE. Best in **bold**, second best underlined (within each cause × sex, separately for RMSE and MAE).

| Cause | Model  | Females       |               | Males         |               |
|-------|--------|---------------|---------------|---------------|---------------|
|       |        | RMSE          | MAE           | RMSE          | MAE           |
| CVD   | DMP-AP | <b>0.0049</b> | 0.0021        | 0.0177        | 0.0057        |
|       | DMP-LC | 0.0142        | 0.0059        | <b>0.0109</b> | 0.0050        |
|       | CoDa   | <u>0.0063</u> | <b>0.0019</b> | <u>0.0145</u> | <b>0.0041</b> |
|       | LC     | 0.0263        | 0.0126        | 0.0233        | 0.0127        |
| EXT   | DMP-AP | 0.0005        | 0.0002        | <u>0.0007</u> | <u>0.0004</u> |
|       | DMP-LC | <u>0.0004</u> | <u>0.0002</u> | <b>0.0005</b> | <b>0.0003</b> |
|       | CoDa   | 0.0007        | 0.0003        | 0.0008        | 0.0004        |
|       | LC     | <b>0.0003</b> | <b>0.0002</b> | 0.0007        | 0.0004        |
| INF   | DMP-AP | 0.0010        | 0.0003        | <u>0.0010</u> | <u>0.0005</u> |
|       | DMP-LC | 0.0018        | 0.0007        | 0.0018        | 0.0008        |
|       | CoDa   | <b>0.0002</b> | <b>0.0001</b> | <u>0.0007</u> | <u>0.0002</u> |
|       | LC     | <u>0.0004</u> | <u>0.0001</u> | <b>0.0004</b> | <b>0.0002</b> |

continued on next page

| Cause | Model  | Females       |               | Males         |               |
|-------|--------|---------------|---------------|---------------|---------------|
|       |        | RMSE          | MAE           | RMSE          | MAE           |
| NEOP  | DMP-AP | 0.0026        | 0.0012        | <u>0.0027</u> | <u>0.0013</u> |
|       | DMP-LC | 0.0012        | 0.0006        | 0.0028        | 0.0015        |
|       | CoDa   | <b>0.0006</b> | <b>0.0003</b> | <b>0.0022</b> | <b>0.0010</b> |
|       | LC     | <u>0.0009</u> | <u>0.0006</u> | 0.0030        | 0.0019        |
| OTHER | DMP-AP | <u>0.0094</u> | 0.0037        | 0.0109        | 0.0038        |
|       | DMP-LC | 0.0131        | 0.0047        | <u>0.0091</u> | <u>0.0037</u> |
|       | CoDa   | <b>0.0060</b> | <b>0.0021</b> | <b>0.0086</b> | <b>0.0031</b> |
|       | LC     | 0.0126        | <u>0.0035</u> | 0.0613        | 0.0251        |
| RESP  | DMP-AP | 0.0073        | 0.0024        | <u>0.0048</u> | <u>0.0018</u> |
|       | DMP-LC | 0.0059        | 0.0021        | 0.0062        | 0.0025        |
|       | CoDa   | <b>0.0031</b> | <b>0.0010</b> | <b>0.0043</b> | <b>0.0016</b> |
|       | LC     | <u>0.0048</u> | <u>0.0019</u> | 0.0058        | 0.0018        |

France exhibits a similar pattern in Table 12. For males, DMP-LC is again broadly strong across causes and is best in several major cells (e.g., CVD and OTHER). For females, CoDa can be extremely competitive in some causes (notably CVD and OTHER), as reflected in the averages across causes. However, this cause-level strength does not translate into good total-mortality performance in a rate-based evaluation, reinforcing a key point: methods can optimise different aspects of the problem (level versus composition), and superior cause-level fit does not automatically imply superior system-level coherence/accuracy on totals.

Table 12: France – Out-of-sample performance by cause and model, train from 1979, with sex shown as column groups. Lower is better for RMSE/MAE. Best in **bold**, second best underlined (within each cause × sex, separately for RMSE and MAE).

| Cause | Model  | Females       |               | Males         |               |
|-------|--------|---------------|---------------|---------------|---------------|
|       |        | RMSE          | MAE           | RMSE          | MAE           |
| CVD   | DMP-AP | 0.0466        | 0.0123        | 0.0122        | 0.0045        |
|       | DMP-LC | <u>0.0058</u> | <u>0.0025</u> | <b>0.0069</b> | <b>0.0030</b> |

continued on next page

| Cause | Model  | Females       |               | Males         |               |
|-------|--------|---------------|---------------|---------------|---------------|
|       |        | RMSE          | MAE           | RMSE          | MAE           |
| EXT   | CoDa   | <b>0.0031</b> | <b>0.0010</b> | 0.0154        | <u>0.0049</u> |
|       | LC     | 0.0229        | 0.0110        | <u>0.0227</u> | 0.0119        |
|       | DMP-AP | 0.0105        | 0.0024        | 0.0022        | 0.0008        |
|       | DMP-LC | <u>0.0015</u> | <u>0.0006</u> | <b>0.0014</b> | <b>0.0005</b> |
|       | CoDa   | <b>0.0013</b> | <b>0.0005</b> | <u>0.0021</u> | <u>0.0007</u> |
| INF   | LC     | 0.0039        | 0.0018        | 0.0021        | 0.0013        |
|       | DMP-AP | 0.0027        | 0.0007        | 0.0014        | 0.0005        |
|       | DMP-LC | <b>0.0006</b> | <b>0.0002</b> | <u>0.0007</u> | <u>0.0003</u> |
|       | CoDa   | <u>0.0015</u> | <u>0.0005</u> | 0.0020        | 0.0006        |
| NEOP  | LC     | 0.0982        | 0.0139        | <b>0.0006</b> | <b>0.0003</b> |
|       | DMP-AP | 0.0209        | 0.0064        | 0.0050        | 0.0020        |
|       | DMP-LC | 0.0013        | <u>0.0006</u> | 0.0028        | <u>0.0014</u> |
|       | CoDa   | <u>0.0010</u> | <b>0.0006</b> | <b>0.0027</b> | <b>0.0009</b> |
| OTHER | LC     | <b>0.0010</b> | 0.0006        | <u>0.0038</u> | 0.0024        |
|       | DMP-AP | 0.0459        | 0.0114        | 0.0064        | 0.0025        |
|       | DMP-LC | 0.0058        | 0.0019        | <b>0.0029</b> | <b>0.0010</b> |
|       | CoDa   | <b>0.0026</b> | <b>0.0009</b> | 0.0079        | 0.0029        |
| RESP  | LC     | <u>0.0092</u> | <u>0.0033</u> | <u>0.0042</u> | <u>0.0020</u> |
|       | DMP-AP | 0.0128        | 0.0026        | <b>0.0059</b> | <b>0.0015</b> |
|       | DMP-LC | <b>0.0042</b> | <b>0.0012</b> | 0.0073        | <u>0.0020</u> |
|       | CoDa   | 0.0065        | <u>0.0017</u> | 0.0097        | 0.0026        |
|       | LC     | <u>0.0044</u> | 0.0017        | <u>0.0072</u> | 0.0026        |

Tables 13 and 14 further clarify these trade-offs. In the U.S., CoDa attains the lowest mean RMSE/MAE for females and is also best on the mean metrics for males, while DMP-AP/DMP-LC remain close competitors. In France, CoDa yields the lowest mean errors across causes for females, whereas DMP-LC is best overall for males. These results suggest that when one aggregates

uniformly across causes, compositional methods can excel; nevertheless, the totals tell a different story, and the coherent Bayesian LC formulation is the only approach that is consistently strong on the full system (accurate totals plus a coherent decomposition).

Table 13: U.S. – OOS mean performance across causes, train from 1979, by sex. Lower is better. Best in **bold**, second best underlined (within each sex, separately for RMSE mean and MAE mean).

| Sex     | Model  | RMSE mean     | MAE mean      |
|---------|--------|---------------|---------------|
| Females | DMP-AP | <u>0.0043</u> | <u>0.0017</u> |
|         | DMP-LC | 0.0061        | 0.0024        |
|         | CoDa   | <b>0.0028</b> | <b>0.0010</b> |
|         | LC     | 0.0076        | 0.0031        |
| Males   | DMP-AP | 0.0063        | <u>0.0023</u> |
|         | DMP-LC | <u>0.0052</u> | 0.0023        |
|         | CoDa   | <b>0.0052</b> | <b>0.0017</b> |
|         | LC     | 0.0158        | 0.0070        |

Table 14: France – OOS mean performance across causes, train from 1979, by sex. Lower is better. Best in **bold**, second best underlined (within each sex, separately for RMSE mean and MAE mean).

| Sex     | Model  | RMSE mean     | MAE mean      |
|---------|--------|---------------|---------------|
| Females | DMP-AP | <u>0.0232</u> | 0.0060        |
|         | DMP-LC | 0.0032        | <u>0.0012</u> |
|         | CoDa   | <b>0.0027</b> | <b>0.0009</b> |
|         | LC     | 0.0233        | 0.0054        |
| Males   | DMP-AP | <u>0.0055</u> | 0.0020        |
|         | DMP-LC | <b>0.0037</b> | <b>0.0014</b> |
|         | CoDa   | 0.0066        | <u>0.0021</u> |
|         | LC     | 0.0067        | 0.0034        |

Figures 5-8 provide visual checks of these results by showing observed log mortality rates, fitted trajectories, and forecast behaviour for selected ages (20, 40, 60, 80), with the dashed line marking the transition from in-sample (1979-2008) to OOS forecasting (2008 onward).

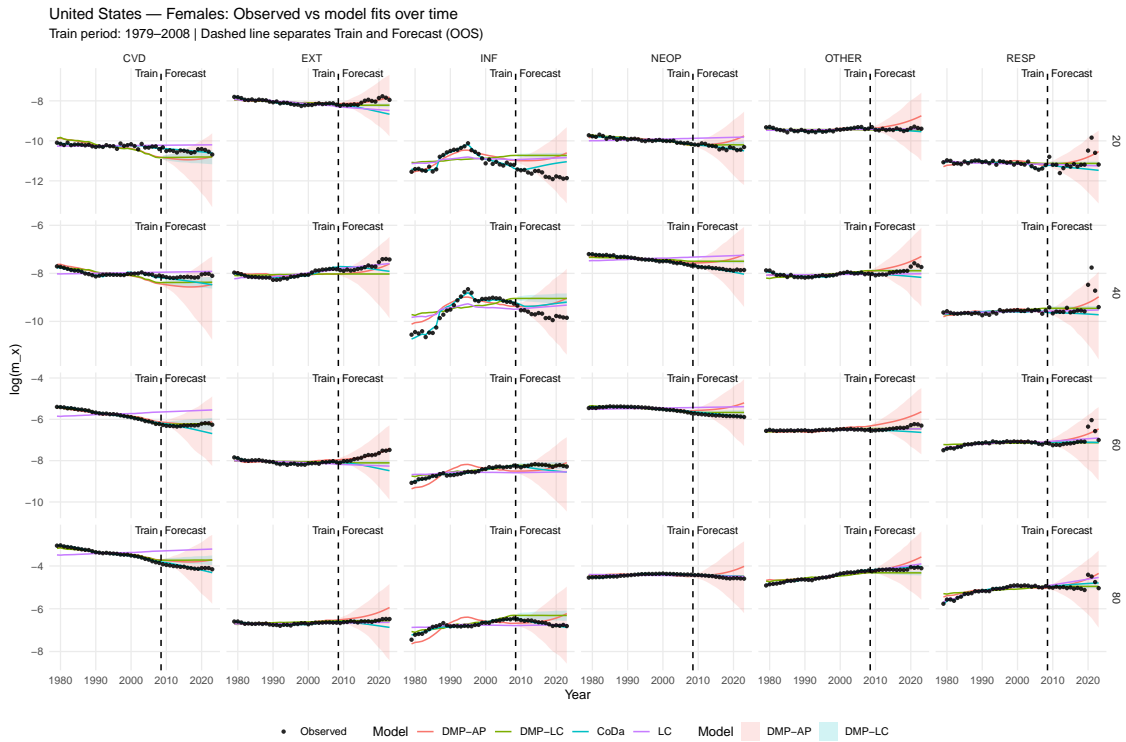


Figure 5: U.S. Female: Observed (black points) and fitted/forecast log mortality rates by cause for selected ages (20, 40, 60, 80). The vertical dashed line marks the end of the in-sample period (1979–2008) and the start of the out-of-sample forecasts.

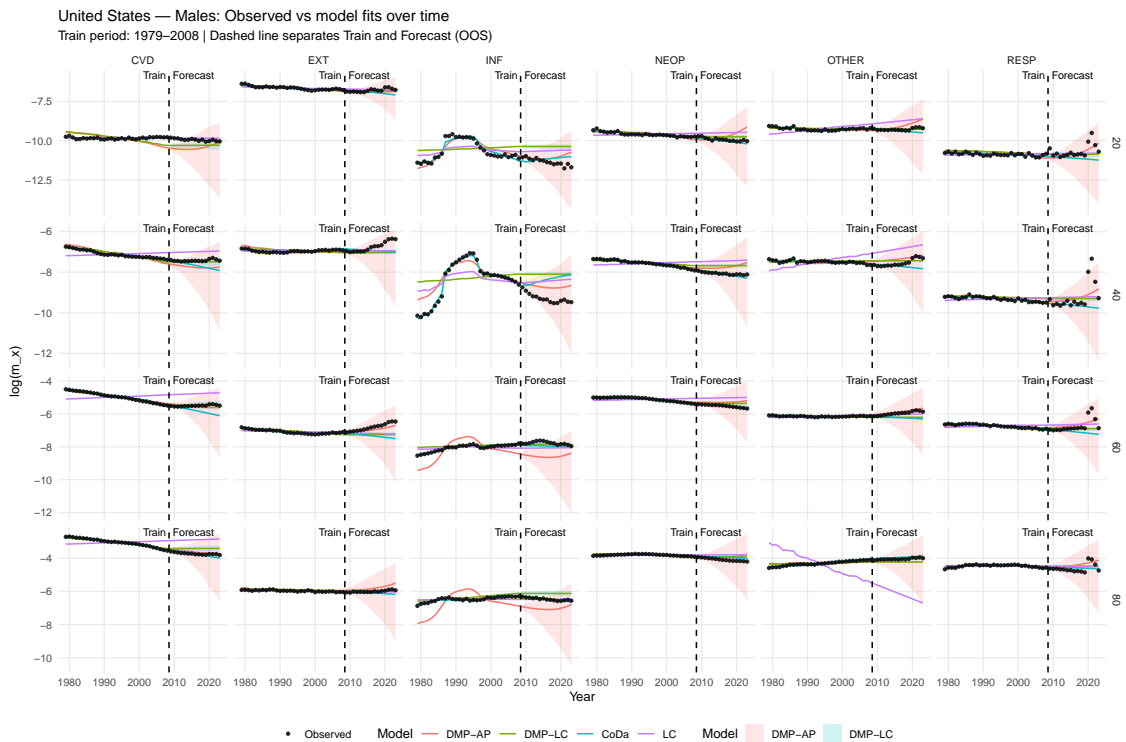


Figure 6: U.S. Male: Observed (black points) and fitted/forecast log mortality rates by cause for selected ages (20, 40, 60, 80). The vertical dashed line marks the end of the in-sample period (1979–2008) and the start of the out-of-sample forecasts.

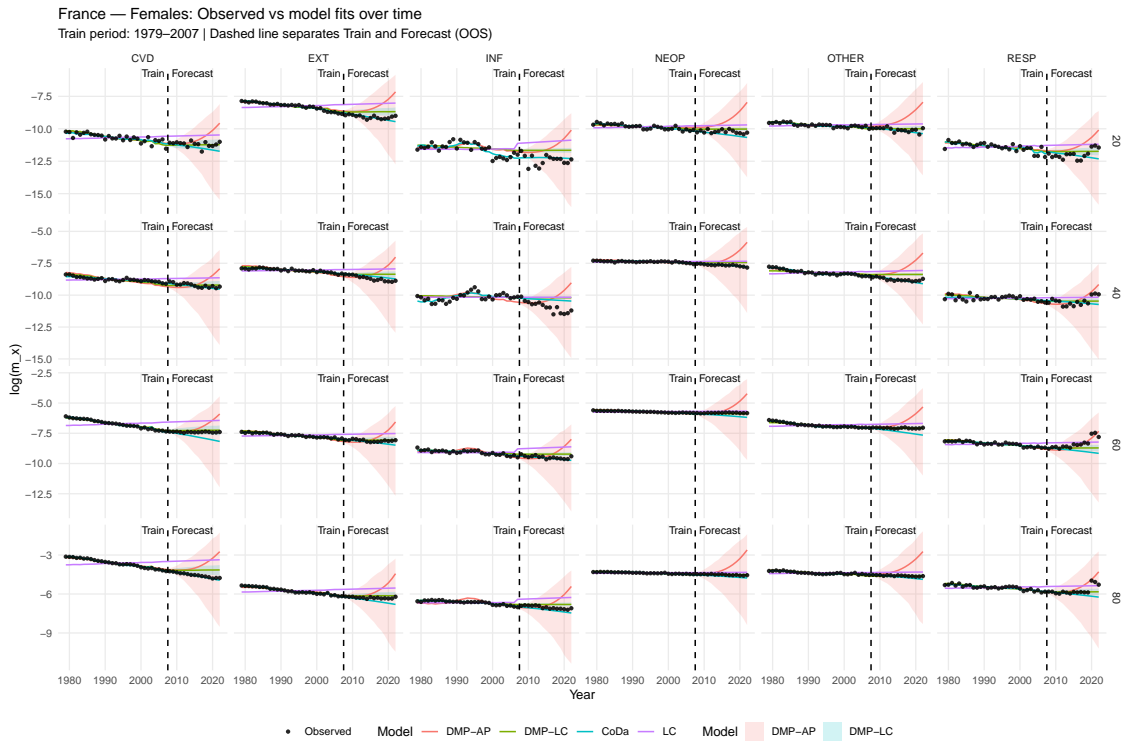


Figure 7: France Female: Observed (black points) and fitted/forecast log mortality rates by cause for selected ages (20, 40, 60, 80). The vertical dashed line marks the end of the in-sample period (1979–2007) and the start of the out-of-sample forecasts.

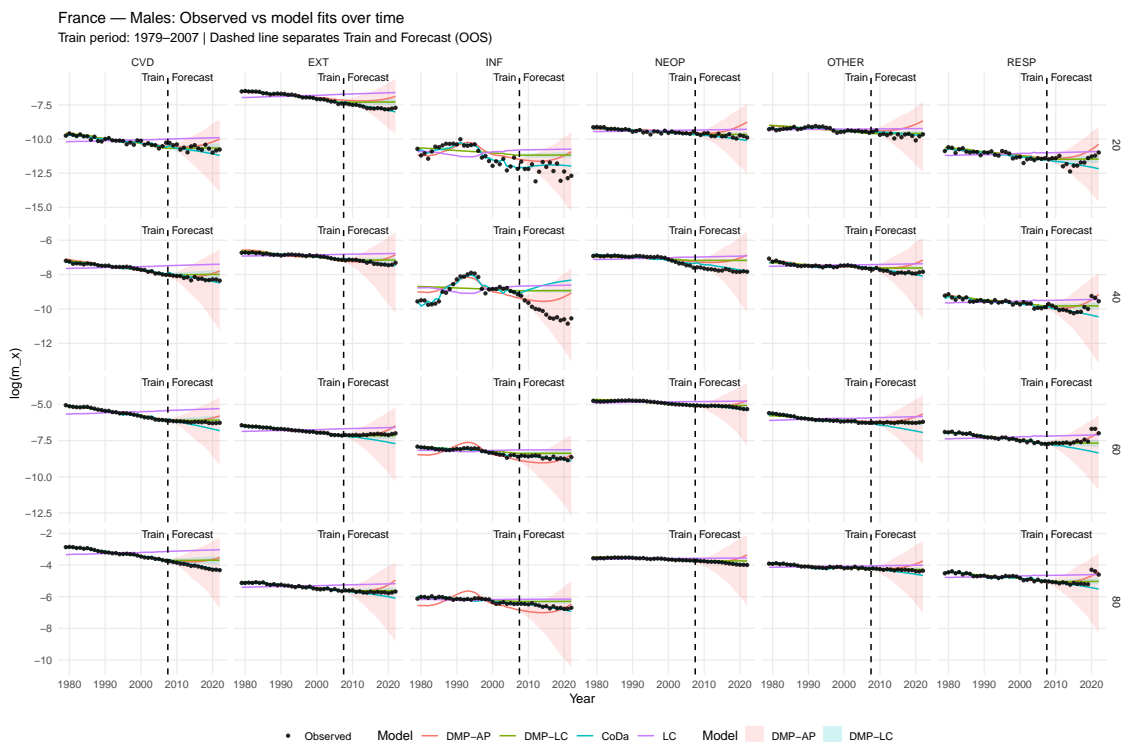


Figure 8: France Male: Observed (black points) and fitted/forecast log mortality rates by cause for selected ages (20, 40, 60, 80). The vertical dashed line marks the end of the in-sample period (1979–2007) and the start of the out-of-sample forecasts.

## B Benchmark models: LC and CoDa

We summarise the two benchmark models used for comparison, i.e. the LC model fitted to cause-specific mortality rates, and a CoDa approach fitted to life-table death distributions. Our implementation follows the specifications in [Kjærgaard et al. \(2019\)](#).

### B.1 Cause-by-cause LC

Let  $D_{t,x,c}$  denote observed deaths in year  $t$ , age group  $x$ , cause  $c$ , and let  $m_{t,x,c}$  be the corresponding (cause-specific) death rate. The LC benchmark is fitted *separately for each cause* using the standard bilinear structure

$$\log m_{t,x,c} = \alpha_{x,c} + \beta_{x,c} \kappa_{t,c} + \varepsilon_{t,x,c},$$

where  $\alpha_{x,c}$  is the average age profile for cause  $c$ ,  $\kappa_{t,c}$  is the time index, and  $\beta_{x,c}$  measures the age-specific sensitivity to changes in  $\kappa_{t,c}$  (with standard identifiability constraints such as  $\sum_x \beta_{x,c} = 1$  and  $\sum_t \kappa_{t,c} = 0$ ). Forecasts are obtained by extrapolating  $\kappa_{t,c}$  (typically with autoregressive integrated moving average (ARIMA)-type time-series models) and then reconstructing  $\hat{m}_{t,x,c}$ .

Because LC is fitted independently by cause, coherence is not guaranteed: in general,  $\sum_c \hat{m}_{t,x,c}$  need not match the independently modelled total. Therefore, we treat LC as a strong but potentially non-coherent baseline ([Wilmoth, 1995](#)).

### B.2 CoDa on life-table death counts

The CoDa benchmark models the distribution of deaths rather than the cause-specific rates. Starting from a multiple-decrement life table, define all-cause life-table deaths  $d_{t,x}$  (for a given radix, such as  $10^5$ ) and transform observed cause-of-death counts into cause-specific life-table deaths via

$$d_{t,x,c} = d_{t,x} \frac{D_{t,x,c}}{D_{t,x}}, \quad \text{where} \quad D_{t,x} = \sum_{c=1}^K D_{t,x,c}.$$

This produces, for each year  $t$ , a nonnegative array  $\{d_{t,x,c}\}$  whose elements sum to the radix, i.e. a composition over the age–cause cells.

To work in an unconstrained space, CoDa applies the centred log-ratio (CLR) transformation. If

we stack the age–cause cells in a single index  $j \in \{1, \dots, NK\}$ , where  $N$  is the number of age groups and  $K$  is the number of causes, and write  $d_{t,j}$ , the CLR is

$$\text{clr}(d_{t,j}) = \log\left(\frac{d_{t,j}}{g_t}\right), \quad g_t = \left(\prod_{j=1}^{NK} d_{t,j}\right)^{1/(NK)}.$$

The transformed series is then decomposed by singular value decomposition, yielding an LC-type factorisation on the CLR scale:

$$\text{clr}(d_{t,j}) = \alpha_j + \sum_{p=1}^P \beta_{j,p} k_{t,p} + \varepsilon_{t,j}.$$

Forecasts are produced by time-series extrapolation (e.g. ARIMA) of the score vectors  $k_{t,p}$ , followed by an inverse-CLR map and closure back to the simplex (so that the predicted death distribution sums to the radix). In the notation of compositional operations, the back-transformation can be written schematically as

$$\widehat{\mathbf{d}}_t = \text{clr}^{-1}\left(\sum_{p=1}^P \beta_p \widehat{k}_{t,p}\right) \oplus \boldsymbol{\alpha},$$

where  $\boldsymbol{\alpha}$  is the baseline (time-average) age–cause death composition, and  $\text{clr}^{-1}(\cdot)$  includes the closure operator that ensures the sum constraint.

## C Posterior summary

In Tables 15 and 16, we present posterior summaries for scalar parameters of the Bayesian AP and LC models, by sex and in-sample years for France and the U.S., respectively.

Table 15: France – Posterior summary for scalar parameters (DMP-AP and DMP-LC), by sex and in-sample start year (1979 vs 1989).

| Year          | Parameter        | Males  |       |        |        |        |                  |           | Females |        |         |         |         |                  |           |
|---------------|------------------|--------|-------|--------|--------|--------|------------------|-----------|---------|--------|---------|---------|---------|------------------|-----------|
|               |                  | Mean   | SD    | 5%     | 50%    | 95%    | $n_{\text{eff}}$ | $\hat{R}$ | Mean    | SD     | 5%      | 50%     | 95%     | $n_{\text{eff}}$ | $\hat{R}$ |
| <b>DMP-AP</b> |                  |        |       |        |        |        |                  |           |         |        |         |         |         |                  |           |
| 1979          | $\nu_0$          | -4.72  | 0.00  | -4.72  | -4.72  | -4.71  | 2923             | 1.00      | -5.36   | 0.00   | -5.36   | -5.36   | -5.36   | 4465             | 1.00      |
|               | $\sigma_\delta$  | 0.67   | 0.11  | 0.52   | 0.65   | 0.86   | 667              | 1.01      | 0.60    | 0.10   | 0.46    | 0.59    | 0.78    | 178              | 1.00      |
|               | $\sigma_\pi$     | 0.03   | 0.00  | 0.03   | 0.03   | 0.04   | 860              | 1.01      | 0.05    | 0.01   | 0.04    | 0.05    | 0.07    | 204              | 1.02      |
|               | $\sigma_\zeta$   | 0.32   | 0.02  | 0.28   | 0.32   | 0.36   | 618              | 1.00      | 0.28    | 0.02   | 0.25    | 0.28    | 0.32    | 211              | 1.01      |
|               | $\sigma_\lambda$ | 0.02   | 0.00  | 0.02   | 0.02   | 0.03   | 508              | 1.01      | 0.02    | 0.00   | 0.01    | 0.02    | 0.02    | 173              | 1.03      |
|               | $\phi$           | 652.72 | 21.87 | 616.82 | 652.82 | 688.93 | 684              | 1.00      | 898.07  | 34.90  | 844.81  | 895.57  | 958.71  | 167              | 1.03      |
| <b>DMP-LC</b> |                  |        |       |        |        |        |                  |           |         |        |         |         |         |                  |           |
| 1979          | $\nu_0$          | -4.73  | 0.00  | -4.73  | -4.73  | -4.73  | 3798             | 1.00      | -5.38   | 0.00   | -5.38   | -5.38   | -5.38   | 3106             | 1.00      |
|               | $\sigma_\kappa$  | 0.65   | 0.09  | 0.53   | 0.64   | 0.81   | 522              | 1.00      | 0.81    | 0.10   | 0.66    | 0.80    | 0.99    | 445              | 1.01      |
|               | $\sigma_\zeta$   | 0.31   | 0.02  | 0.27   | 0.30   | 0.35   | 438              | 1.00      | 0.28    | 0.02   | 0.24    | 0.27    | 0.31    | 387              | 1.01      |
|               | $\phi$           | 390.58 | 11.25 | 372.88 | 390.25 | 409.77 | 597              | 1.01      | 667.74  | 23.44  | 629.35  | 667.30  | 707.14  | 268              | 1.01      |
| <b>DMP-AP</b> |                  |        |       |        |        |        |                  |           |         |        |         |         |         |                  |           |
| 1989          | $\nu_0$          | -4.83  | 0.00  | -4.83  | -4.83  | -4.83  | 4608             | 1.00      | -5.48   | 0.00   | -5.48   | -5.48   | -5.48   | 5609             | 1.00      |
|               | $\sigma_\delta$  | 0.66   | 0.11  | 0.51   | 0.64   | 0.87   | 631              | 1.00      | 0.60    | 0.11   | 0.46    | 0.58    | 0.80    | 366              | 1.02      |
|               | $\sigma_\pi$     | 0.04   | 0.01  | 0.03   | 0.04   | 0.05   | 850              | 1.01      | 0.06    | 0.01   | 0.05    | 0.06    | 0.08    | 412              | 1.00      |
|               | $\sigma_\zeta$   | 0.34   | 0.03  | 0.30   | 0.34   | 0.39   | 711              | 1.00      | 0.31    | 0.02   | 0.28    | 0.31    | 0.35    | 496              | 1.00      |
|               | $\sigma_\lambda$ | 0.03   | 0.00  | 0.03   | 0.03   | 0.04   | 545              | 1.00      | 0.03    | 0.00   | 0.02    | 0.03    | 0.03    | 379              | 1.01      |
|               | $\phi$           | 839.40 | 36.75 | 781.70 | 838.02 | 902.39 | 595              | 1.00      | 2032.95 | 130.66 | 1832.24 | 2027.17 | 2256.96 | 433              | 1.01      |
| <b>DMP-LC</b> |                  |        |       |        |        |        |                  |           |         |        |         |         |         |                  |           |
| 1989          | $\nu_0$          | -4.84  | 0.00  | -4.84  | -4.84  | -4.84  | 2400             | 1.00      | -5.49   | 0.00   | -5.49   | -5.49   | -5.49   | 4425             | 1.00      |
|               | $\sigma_\kappa$  | 0.75   | 0.12  | 0.58   | 0.74   | 0.97   | 285              | 1.01      | 0.89    | 0.13   | 0.71    | 0.88    | 1.12    | 447              | 1.00      |
|               | $\sigma_\zeta$   | 0.34   | 0.03  | 0.30   | 0.34   | 0.39   | 229              | 1.00      | 0.31    | 0.02   | 0.27    | 0.30    | 0.35    | 350              | 1.01      |
|               | $\phi$           | 634.99 | 24.50 | 593.58 | 635.33 | 675.55 | 194              | 1.01      | 1316.73 | 74.93  | 1195.37 | 1316.18 | 1441.40 | 610              | 1.00      |

Table 16: U.S. – Posterior summary for scalar parameters (DMP-AP and DMP-LC), by sex and in-sample start year (1979 vs 1989).

| Year                 | Parameter        | Males  |       |        |        |        |                  |           | Females |       |        |        |        |                  |           |
|----------------------|------------------|--------|-------|--------|--------|--------|------------------|-----------|---------|-------|--------|--------|--------|------------------|-----------|
|                      |                  | Mean   | SD    | 5%     | 50%    | 95%    | $n_{\text{eff}}$ | $\hat{R}$ | Mean    | SD    | 5%     | 50%    | 95%    | $n_{\text{eff}}$ | $\hat{R}$ |
| <b><u>DMP-AP</u></b> |                  |        |       |        |        |        |                  |           |         |       |        |        |        |                  |           |
| 1979                 | $\nu_0$          | -4.65  | 0.00  | -4.65  | -4.65  | -4.65  | 2674             | 1.00      | -5.18   | 0.00  | -5.18  | -5.18  | -5.18  | 2990             | 1.00      |
|                      | $\sigma_\delta$  | 0.70   | 0.12  | 0.54   | 0.68   | 0.91   | 323              | 1.00      | 0.63    | 0.11  | 0.48   | 0.62   | 0.84   | 195              | 1.02      |
|                      | $\sigma_\pi$     | 0.02   | 0.00  | 0.01   | 0.02   | 0.02   | 210              | 1.00      | 0.02    | 0.00  | 0.02   | 0.02   | 0.03   | 264              | 1.00      |
|                      | $\sigma_\zeta$   | 0.34   | 0.03  | 0.30   | 0.34   | 0.39   | 269              | 1.03      | 0.32    | 0.03  | 0.28   | 0.32   | 0.37   | 225              | 1.00      |
|                      | $\sigma_\lambda$ | 0.03   | 0.00  | 0.02   | 0.03   | 0.04   | 249              | 1.00      | 0.01    | 0.00  | 0.01   | 0.01   | 0.02   | 96               | 1.04      |
|                      | $\phi$           | 483.17 | 12.47 | 462.16 | 483.03 | 503.70 | 217              | 1.00      | 591.35  | 16.80 | 562.09 | 591.38 | 618.97 | 242              | 1.01      |
| <b><u>DMP-LC</u></b> |                  |        |       |        |        |        |                  |           |         |       |        |        |        |                  |           |
| 1979                 | $\nu_0$          | -4.66  | 0.00  | -4.66  | -4.66  | -4.66  | 3172             | 1.00      | -5.18   | 0.00  | -5.18  | -5.18  | -5.18  | 2328             | 1.00      |
|                      | $\sigma_\kappa$  | 0.37   | 0.05  | 0.30   | 0.37   | 0.46   | 273              | 1.01      | 0.31    | 0.04  | 0.25   | 0.31   | 0.39   | 340              | 1.00      |
|                      | $\sigma_\zeta$   | 0.33   | 0.02  | 0.29   | 0.33   | 0.37   | 186              | 1.00      | 0.32    | 0.02  | 0.28   | 0.31   | 0.36   | 290              | 1.02      |
|                      | $\phi$           | 229.22 | 5.85  | 219.36 | 229.40 | 238.45 | 298              | 1.01      | 416.47  | 10.76 | 398.33 | 416.54 | 434.21 | 275              | 1.01      |
| <b><u>DMP-AP</u></b> |                  |        |       |        |        |        |                  |           |         |       |        |        |        |                  |           |
| 1989                 | $\nu_0$          | -4.72  | 0.00  | -4.72  | -4.72  | -4.72  | 2549             | 1.00      | -5.22   | 0.00  | -5.22  | -5.22  | -5.22  | 2984             | 1.00      |
|                      | $\sigma_\delta$  | 0.71   | 0.12  | 0.54   | 0.70   | 0.94   | 387              | 1.01      | 0.64    | 0.11  | 0.49   | 0.62   | 0.85   | 258              | 1.03      |
|                      | $\sigma_\pi$     | 0.02   | 0.00  | 0.01   | 0.02   | 0.03   | 425              | 1.00      | 0.02    | 0.00  | 0.02   | 0.02   | 0.03   | 378              | 1.01      |
|                      | $\sigma_\zeta$   | 0.35   | 0.03  | 0.31   | 0.35   | 0.40   | 254              | 1.00      | 0.32    | 0.02  | 0.29   | 0.32   | 0.36   | 346              | 1.02      |
|                      | $\sigma_\lambda$ | 0.03   | 0.00  | 0.02   | 0.03   | 0.03   | 286              | 1.02      | 0.02    | 0.00  | 0.01   | 0.02   | 0.02   | 231              | 1.01      |
|                      | $\phi$           | 615.65 | 21.02 | 579.38 | 615.89 | 649.42 | 510              | 1.00      | 928.29  | 31.49 | 876.75 | 928.39 | 980.45 | 426              | 1.01      |
| <b><u>DMP-LC</u></b> |                  |        |       |        |        |        |                  |           |         |       |        |        |        |                  |           |
| 1989                 | $\nu_0$          | -4.72  | 0.00  | -4.72  | -4.72  | -4.72  | 2842             | 1.00      | -5.23   | 0.00  | -5.23  | -5.23  | -5.22  | 3424             | 1.00      |
|                      | $\sigma_\kappa$  | 0.44   | 0.08  | 0.34   | 0.43   | 0.59   | 491              | 1.01      | 0.31    | 0.05  | 0.24   | 0.30   | 0.40   | 232              | 1.02      |
|                      | $\sigma_\zeta$   | 0.35   | 0.03  | 0.31   | 0.35   | 0.39   | 467              | 1.00      | 0.32    | 0.02  | 0.29   | 0.32   | 0.36   | 291              | 1.00      |
|                      | $\phi$           | 545.39 | 18.20 | 516.78 | 545.21 | 574.64 | 472              | 1.00      | 805.97  | 28.19 | 759.64 | 805.95 | 851.91 | 273              | 1.00      |